



LJMU Research Online

Nater, A, Mattle-Greminger, M, Nurcahyo, A, Nowak, M, de Manuel, M, Desai, T, Groves, C, Pybus, M, Sonay, T, Roos, C, Lameira, AR, Wich, SA, Askew, J, Davila-Ross, M, Fredriksson, G, de Valles, G, Casals, F, Prado-Martinez, J, Goosens, B, Verschoor, EJ, Warren, KS, Singleton, I, Marques, DA, Pamungkas, J, Perwitasari-Farajallah, D, Rianti, P, Tuuga, A, Gut, IG, Gut, M, Orozco-terWengel, P, van Schaik, CP, Bertranpetit, J, Anisimova, M, Scally, A, Marques-Bonet, T, Meijaard, E and Krutzen, M

Morphometric, Behavioral, and Genomic Evidence for a New Orangutan Species

<http://researchonline.ljmu.ac.uk/7484/>

Article

Citation (please note it is advisable to refer to the publisher's version if you intend to cite from this work)

Nater, A, Mattle-Greminger, M, Nurcahyo, A, Nowak, M, de Manuel, M, Desai, T, Groves, C, Pybus, M, Sonay, T, Roos, C, Lameira, AR, Wich, SA, Askew, J, Davila-Ross, M, Fredriksson, G, de Valles, G, Casals, F, Prado-Martinez, J, Goosens, B, Verschoor, EJ, Warren, KS, Sinaleton, I, Marques, DA.

LJMU has developed [LJMU Research Online](http://researchonline.ljmu.ac.uk/) for users to access the research output of the University more effectively. Copyright © and Moral Rights for the papers on this site are retained by the individual authors and/or other copyright owners. Users may download and/or print one copy of any article(s) in LJMU Research Online to facilitate their private study or for non-commercial research. You may not engage in further distribution of the material or use it for any profit-making activities or any commercial gain.

The version presented here may differ from the published version or from the version of the record. Please see the repository URL above for details on accessing the published version and note that access may require a subscription.

<http://researchonline.ljmu.ac.uk/>

For more information please contact researchonline@ljmu.ac.uk

<http://researchonline.ljmu.ac.uk/>

A NEW SPECIES OF ORANGUTAN

1 **Report**2 **Morphometric, behavioral, and genomic evidence**
3 **for a new orangutan species**

4 **Authors:** Alexander Nater^{1,2,3§*}, Maja P. Mattle-Greminger^{1,2§}, Anton Nurcahyo^{4§}, Matthew G.
5 Nowak^{5,6§}, Marc de Manuel⁷, Tariq Desai⁸, Colin Groves⁴, Marc Pybus⁷, Tugce Bilgin Sonay¹, Christian
6 Roos⁹, Adriano R. Lameira^{10,11}, Serge A. Wich^{12,13}, James Askew¹⁴, Marina Davila-Ross¹⁵, Gabriella
7 Fredriksson^{5,13}, Guillem de Valles⁷, Ferran Casals¹⁶, Javier Prado-Martinez¹⁷, Benoit Goossens^{18,19,20,21},
8 Ernst J. Verschoor²², Kristin S. Warren²³, Ian Singleton^{5,24}, David A. Marques^{1,25}, Joko Pamungkas^{26,27},
9 Dyah Perwitasari-Farajallah^{26,28}, Puji Rianti^{28,26,1}, Augustine Tuuga²⁰, Ivo G. Gut^{29,30}, Marta Gut^{29,30},
10 Pablo Orozco-terWengel¹⁸, Carel P. van Schaik¹, Jaume Bertranpetit^{7,31}, Maria Anisimova^{32,33}, Aylwyn
11 Scally⁸, Tomas Marques-Bonet^{7,29,34}, Erik Meijaard^{4,35*} and Michael Krützen *

12 §These authors contributed equally to this work.

13 *Correspondence to: michael.krutzen@aim.uzh.ch (MK, lead contact), alexander.nater@uzh.ch (AIN),
14 emeijaard@gmail.com (EM),

15 **Affiliations:**

16 ¹Evolutionary Genetics Group, Department of Anthropology, University of Zurich, Winterthurerstrasse
17 190, 8057 Zürich, Switzerland.

18 ²Department of Evolutionary Biology and Environmental Studies, University of Zurich,
19 Winterthurerstrasse 190, 8057 Zürich, Switzerland.

20 ³Lehrstuhl für Zoologie und Evolutionsbiologie, Department of Biology, University of Konstanz,
21 Universitätsstrasse 10, 78457 Konstanz, Germany.

22 ⁴School of Archaeology and Anthropology, Australian National University, Canberra, Australia.

23 ⁵Sumatran Orangutan Conservation Programme (PanEco-YEL), Jalan Wahid Hasyim 51/74, Medan
24 20154, Indonesia

25 ⁶Department of Anthropology, Southern Illinois University, 1000 Faner Drive, Carbondale, IL 62901,
26 USA.

27 ⁷Institut de Biologia Evolutiva (UPF-CSIC), Universitat Pompeu Fabra, Doctor Aiguader 88, Barcelona
28 08003, Spain.

29 ⁸Department of Genetics, University of Cambridge, Downing Street, Cambridge, CB2 3EH, UK.

A NEW SPECIES OF ORANGUTAN

30 ⁹Gene Bank of Primates and Primate Genetics Laboratory, German Primate Center, Leibniz Institute for
31 Primate Research, 37077 Göttingen, Germany.

32 ¹⁰Department of Anthropology, Durham University, Dawson Building, South Road, Durham, DH1 3LE,
33 UK.

34 ¹¹School of Psychology & Neuroscience, St. Andrews University, St Mary's Quad, South Street, St.
35 Andrews, Fife, KY16 9JP, Scotland, United Kingdom.

36 ¹²School of Natural Sciences and Psychology, Liverpool John Moores University, James Parsons
37 Building, Byrom Street, L33AF Liverpool, UK.

38 ¹³Institute for Biodiversity and Ecosystem Dynamics, University of Amsterdam, Sciencepark 904,
39 Amsterdam 1098, Netherlands.

40 ¹⁴Department of Biological Sciences, University of Southern California, 3616 Trousdale Parkway, Los
41 Angeles, CA 90089, USA.

42 ¹⁵Department of Psychology, University of Portsmouth, King Henry Building, King Henry 1st Street,
43 Portsmouth, PO1 2DY, UK.

44 ¹⁶Servei de Genòmica, Universitat Pompeu Fabra, Doctor Aiguader 88, Barcelona 08003, Spain.

45 ¹⁷Wellcome Trust Sanger Institute, Wellcome Trust Genome Campus, Hinxton CB10 1SA, UK.

46 ¹⁸School of Biosciences, Cardiff University, Sir Martin Evans Building, Museum Avenue, Cardiff CF10
47 3AX, UK.

48 ¹⁹Danau Girang Field Centre, c/o Sabah Wildlife Department, Wisma Muis, 88100 Kota Kinabalu,
49 Sabah, Malaysia.

50 ²⁰Sabah Wildlife Department, Wisma Muis, 88100 Kota Kinabalu, Sabah, Malaysia.

51 ²¹Sustainable Places Research Institute, Cardiff University, 33 Park Place, Cardiff CF10 3BA, UK.

52 ²²Department of Virology, Biomedical Primate Research Centre, Lange Kleiweg 161, 2288GJ Rijswijk,
53 The Netherlands.

54 ²³Conservation Medicine Program, College of Veterinary Medicine, Murdoch University, South Street,
55 Murdoch 6150, Australia.

56 ²⁴Foundation for a Sustainable Ecosystem (YEL), Medan, Indonesia.

57 ²⁵Institute of Ecology and Evolution, University of Bern, Baltzerstrasse 6, 3012 Bern, Switzerland.

58 ²⁶Primate Research Center, Bogor Agricultural University, Bogor 16151, Indonesia.

59 ²⁷Faculty of Veterinary Medicine, Bogor Agricultural University, Darmaga Campus, Bogor 16680,
60 Indonesia.

A NEW SPECIES OF ORANGUTAN

61 ²⁸Animal Biosystematics and Ecology Division, Department of Biology, Bogor Agricultural University,
62 Jalan Agatis, Dramaga Campus, Bogor 16680, Indonesia.

63 ²⁹CNAG-CRG, Centre for Genomic Regulation (CRG), Barcelona Institute of Science and Technology
64 (BIST), Baldiri i Reixac 4, Barcelona 08028, Spain.

65 ³⁰Universitat Pompeu Fabra (UPF), Plaça de la Mercè, 10, 08002 Barcelona, Spain.

66 ³¹Leverhulme Centre for Human Evolutionary Studies, Department of Archaeology and Anthropology,
67 University of Cambridge, Cambridge, UK.

68 ³²Institute of Applied Simulations, School of Life Sciences and Facility Management, Zurich University
69 of Applied Sciences ZHAW, Einsiedlerstrasse 31a, 8820 Wädenswil, Switzerland.

70 ³³Swiss Institute of Bioinformatics, Quartier Sorge - Batiment Genopode, 1015 Lausanne, Switzerland.

71 ³⁴Institucio Catalana de Recerca i Estudis Avançats (ICREA), Barcelona 08010, Spain.

72 ³⁵Borneo Futures, Bandar Seri Begawan, Brunei Darussalam.

Uncorrected proof -
Under embargo until 02NOV17 12PM ET
-Do not distribute without permission-

73 **Summary**

74 Six extant species of non-human great apes are currently recognized: Sumatran and Bornean orangutans,
75 eastern and western gorillas, and chimpanzees and bonobos [1]. However, large gaps remain in our
76 knowledge of fine-scale variation in hominoid morphology, behavior, and genetics, and aspects of great
77 ape taxonomy remain in flux. This is particularly true for orangutans (genus: *Pongo*), the only Asian
78 great apes, and phylogenetically our most distant relatives among extant hominids [1]. Designation of
79 Bornean and Sumatran orangutans, *P. pygmaeus* (Linnaeus 1760) and *P. abelii* (Lesson 1827), as distinct
80 species occurred in 2001 [1, 2]. Here, we show that an isolated population from Batang Toru, at the
81 southernmost range of extant Sumatran orangutans south of Lake Toba, is distinct from other northern
82 Sumatran and Bornean populations. By comparing cranio-mandibular and dental characters of an
83 orangutan killed in a human-animal conflict to 33 adult male orangutans of similar developmental stage,
84 we found consistent differences between the Batang Toru individual and other extant Ponginae. A
85 second line of evidence provided our analyses of 37 orangutan genomes. Model-based approaches
86 revealed that the deepest split in the evolutionary history of extant orangutans occurred ~3.38 Ma ago
87 between the Batang Toru population and those to the north of Lake Toba, while both currently
88 recognized species separated much later about 674 ka ago. Our combined analyses support a new
89 classification of orangutans into three extant species. The new species, *Pongo tapanuliensis*,
90 encompasses the Batang Toru population, of which fewer than 800 individuals survive.

Uncorrected proof - 12 PM ET
Under embargo until 02 NOV 17 12 PM ET
-Do not distribute without permission-

91 **Results and Discussion**

92 Despite decades of field studies [3] our knowledge of variation among orangutans remains limited as
 93 many populations occur in isolated and inaccessible habitats, leaving questions regarding their
 94 evolutionary history and taxonomic classification largely unresolved. In particular, Sumatran
 95 populations south of Lake Toba had long been overlooked, even though a 1939 review of the species'
 96 range mentioned that orangutans had been reported in several forest areas in that region [4]. Based on
 97 diverse sources of evidence, we describe a new orangutan species, *Pongo tapanuliensis*, which
 98 encompasses a geographically and genetically isolated population found in the Batang Toru area at the
 99 southernmost range of extant Sumatran orangutans, south of Lake Toba, Indonesia.

100 **Systematics**

101 Genus *Pongo* Lacépède, 1799

102 *Pongo tapanuliensis* sp. nov. Nurcahyo, Meijaard, Nowak, Fredriksson & Groves

103 Tapanuli Orangutan

104 **Etymology.** The species name refers to three North Sumatran districts (North, Central, and South
 105 Tapanuli) to which *P. tapanuliensis* is endemic.

106 **Holotype.** The complete skeleton of an adult male orangutan that died from wounds sustained by local
 107 villagers in November 2013 near Sugi Tonga, Marancar, Tapanuli (Batang Toru) Forest Complex
 108 (1°35'54.1"N, 99°16'36.5"E), South Tapanuli District, North Sumatra, Indonesia. Skull and
 109 postcranium are lodged in the Museum Zoologicum Bogoriense, Indonesia, accession number
 110 MZB39182. High-resolution 3D reconstructions of the skull and mandible are available as
 111 supplementary material.

112 **Paratypes.** Adult individuals of *P. tapanuliensis* (P2591-M435788 – P2591-M435790) photographed
 113 by Tim Laman in the Batang Toru Forest Complex (1°41'9.1"N, 98°59'38.1"E), North Tapanuli
 114 District, North Sumatra, Indonesia. Paratypes are available from <http://www.morphobank.org> (Login:
 115 2591 / Password: tapanuliorangutan).

116 **Differential diagnosis.** We compared the holotype to a comprehensive comparative data set of 33 adult
 117 male orangutans from 10 institutions housing osteological specimens. Unless otherwise stated, all units
 118 are in [mm]. Summary statistics for all measurements are listed in Tables S1–3. *Pongo tapanuliensis*
 119 differs from all extant orangutans in the breadth of the upper canine (21.5 vs. <20.86); the shallow face
 120 depth (6.0 vs. >8.4); the narrower interpterygoid distance (at posterior end of pterygoids 33.8 vs. >43.9;
 121 at anterior end of pterygoids, 33.7 vs. >43.0); the shorter tympanic tube (23.9 vs. >28.4, mostly >30);
 122 the shorter temporomandibular joint (22.5 vs. >24.7); the narrower maxillary incisor row (28.3 vs.
 123 >30.1); the narrower distance across the palate at the first molars (62.7 vs. >65.7); the shorter horizontal

124 length of the mandibular symphysis (49.3 vs. >53.7); the smaller inferior transverse torus (horizontal
 125 length from anterior surface of symphysis 31.8 compared to >36.0); and the width of the ascending
 126 ramus of the mandible (55.9 vs. >56.3).

127 *Pongo tapanuliensis* differs specifically from *P. abelii* by its deep suborbital fossa, triangular pyriform
 128 aperture, and angled facial profile; the longer nuchal surface (70.5 vs. <64.7); the wider rostrum,
 129 posterior to the canines (59.9 vs. <59); the narrower orbits (33.8 vs. <34.6); the shorter (29.2 vs. >30.0)
 130 and narrower foramen magnum (23.2 vs. >23.3); the narrower bicondylar breadth (120.0 vs. >127.2);
 131 the narrower mandibular incisor row (24.4 vs. >28.3); the greater mesio-distal length of the upper canine
 132 (19.44 vs. <17.55). The male long call has a higher maximum frequency range of the roar pulse type (>
 133 800 Hz vs. <747) with a higher ‘shape’ (>952 Hz/s vs. <934).

134 *Pongo tapanuliensis* differs from *P. pygmaeus* by possessing a nearly straight zygomaxillary suture, the
 135 lower orbit (orbit height 33.4 vs. >35.3); the male long call has a longer duration (>111 seconds vs. <90)
 136 with a greater number of pulses (>52 pulses vs. <45), and is delivered at a greater rate (>0.82 pulses per
 137 20 seconds vs. <0.79).

138 *Pongo tapanuliensis* differs specifically from *Pongo ‘pygmaeus’ palaeosumatrensis* in the smaller size
 139 of the first upper molar (mesio-distal length 13.65 vs. >14.0, buccolingual breadth 11.37 vs. >12.10,
 140 crown area 155.2 mm² vs. >175.45, Figure S1).

141 **Description.** Craniometrically, the type skull of *P. tapanuliensis* (Figure 1B) is significantly smaller
 142 than any skull of comparable developmental stage of other orangutans; it falls outside of the interquartile
 143 ranges of *P. abelii* and *P. pygmaeus* for 24 of 39 cranio-mandibular measurements (Table S1). A
 144 principal component analysis (PCA) of 26 cranio-mandibular measurements commonly used in primate
 145 taxonomic classification [5, 6] shows consistent differences between *P. tapanuliensis* and the two
 146 currently recognized species (Figures 1C and S2).

147 The external morphology of *P. tapanuliensis* is more similar to *P. abelii* in its linear body build and
 148 more cinnamon pelage than *P. pygmaeus*. The hair texture of *P. tapanuliensis* is frizzier, contrasting in
 149 particular with the long, loose body hair of *P. abelii*. *Pongo tapanuliensis* has a prominent moustache
 150 and flat flanges covered in downy hair in dominant males, while flanges of older males resemble more
 151 those of Bornean males. Females of *P. tapanuliensis* have beards, unlike *P. pygmaeus*.

152 **Distribution.** *Pongo tapanuliensis* occurs only in a small number of forest fragments in the districts of
 153 Central, North, and South Tapanuli, Indonesia (Figure 1A). The total distribution covers approximately
 154 1,000 km², with an estimated population size of fewer than 800 individuals [7]. The current distribution
 155 of *P. tapanuliensis* is almost completely restricted to medium elevation hill and submontane forest
 156 (~300–1300 m asl) [7-9]. While densities are highest in primary forest, it does occur at lower densities
 157 in mixed agroforest at the edge of primary forest areas [10, 11]. Until relatively recently, *P. tapanuliensis*

158 was more widespread to the south and west of the current distribution, although evidence for this is
159 largely anecdotal [12, 13].

160 Other hominoid species and subspecies were previously described using standard univariate and
161 multivariate techniques to quantify morphological character differences. The elevation of bonobos (*P.*
162 *paniscus*) from a subspecies to a species dates back to Coolidge [14] and was based on summary
163 statistics of primarily morphological data from a single female specimen of *P. paniscus*, five available
164 *P. paniscus* skulls, and comparative data of what is now *P. troglodytes*. Groves and colleagues [5] and
165 Shea et al. [15] supported Coolidge's proposal using larger sample sizes and discriminant function
166 analyses. Shea et al. [15] remarked that the species designation for *P. paniscus*, which was largely based
167 on morphological comparisons, was ultimately strengthened by genetic, ecological, and behavioral data,
168 as we attempted here for *Pongo tapanuliensis*. For the genus *Gorilla*, Stumpf et al. [16] and Groves [17]
169 used cranio-mandibular data from 747 individuals from 19 geographic regions, confirming a
170 classification of the genus into two species (*G. gorilla* and *G. beringei*), as proposed earlier by Groves
171 [1]. Other recent primate species descriptions primarily relied on an inconsistent mix of data on pelage
172 color, ecology, morphology, and/or vocalizations [18-23], with only a few also incorporating genetic
173 analyses [24, 25].

174 Here, we used an integrative approach by corroborating the morphological analysis, behavioral and
175 ecological data with whole-genome data of 37 orangutans with known provenance, covering the entire
176 range of extant orangutans including areas never sampled before (Figure 2A, Table S4). We applied a
177 model-based approach to statistically evaluate competing demographic models, identify independent
178 evolutionary lineages, and infer levels of gene flow and the timing of genetic isolation between lineages.
179 This enabled us to directly compare complex and realistic models of speciation. We refrained from
180 directly comparing genetic differentiation among the three species in the genus *Pongo* with that of other
181 hominoids, as we deem such comparisons problematic in order to evaluate whether *P. tapanuliensis*
182 constitutes a new species. This is because estimates of genetic differentiation reflect a combination of
183 divergence time, demographic history, and gene flow, and are also influenced by the employed genetic
184 marker system [26, 27].

185 A PCA (Figure 2B) of genomic diversity highlighted the divergence between individuals from Borneo
186 and Sumatra (PC1), but also separated *P. tapanuliensis* from *P. abelii* (PC2). The same clustering pattern
187 was also found in a model-based analysis of population structure (Figure 2C), and is consistent with an
188 earlier genetic study analyzing a larger number of non-invasively collected samples using microsatellite
189 markers [28]. However, while powerful in detecting extant population structure, population history and
190 speciation cannot be inferred, as they are not suited to distinguish between old divergences with gene
191 flow and cases of recent divergence with isolation [29, 30]. To address this problem and further

192 investigate the timing of population splits and gene flow, we therefore employed different
193 complementary modeling and phylogenetic approaches.

194 We applied an Approximate Bayesian Computation (ABC) approach, which allows to infer and compare
195 arbitrarily complex demographic modes based on the comparison of the observed genomic data to
196 extensive population genetic simulations [31]. Our analyses revealed three deep evolutionary lineages
197 in extant orangutans (Figures 3A and B). Colonization scenarios in which the earliest split within *Pongo*
198 occurred between the lineages leading to *P. abelii* and *P. tapanuliensis* were much better supported than
199 scenarios in which the earliest split was between Bornean and Sumatran species (models 1 vs. models
200 2, combined posterior probability: 99.91%, Figure 3A). Of the two best scenarios, a model postulating
201 colonization of both northern Sumatra and Borneo from an ancestral population likely situated south of
202 Lake Toba on Sumatra, had the highest support (model 1a vs. model 1b, posterior probability 97.56%,
203 Figure 3A). Our results supported a scenario in which orangutans from mainland Asia first entered
204 Sundaland south of what is now Lake Toba on Sumatra, the most likely entry point based on
205 paleogeographic reconstructions [32]. This ancestral population, of which *P. tapanuliensis* is a direct
206 descendant, then served as a source for the subsequent different colonization events of what is now
207 Borneo, Java and northern Sumatra.

208 We estimated the split time between populations north and south of Lake Toba at ~3.4 Ma (Figure 3B,
209 Table S5). Under our best-fitting model, we found evidence for post-split gene flow across Lake Toba
210 (~0.3–0.9 migrants per generation, Table S5), which is consistent with highly significant signatures of
211 gene flow between *P. abelii* and *P. tapanuliensis* using D-statistics (CK, BT, WA, *Homo sapiens*: $D = -$
212 0.2819 , $p\text{-value} < 0.00001$; WK, BT, LK, *Homo sapiens*: $D = -0.2967$, $p\text{-value} < 0.00001$). Such gene flow
213 resulted in higher autosomal affinity of *P. tapanuliensis* to *P. abelii* compared to *P. pygmaeus* in the
214 PCA (Figure 2B), explaining the smaller amount of variance captured by PC2 (separating *P.*
215 *tapanuliensis* from all other populations) compared to PC1 (separating *P. pygmaeus* from the Sumatran
216 populations). The parameter estimates from a Bayesian full-likelihood analysis implemented in the
217 software G-PhoCS were in good agreement with those obtained by the ABC analysis, although the split
218 time between populations north and south of Lake Toba was more recent (~2.27 Ma, 95%-HPD: 2.21–
219 2.35, Table S5). The G-PhoCS analysis revealed highly asymmetric gene flow between populations
220 north and south of the Toba caldera, with much lower levels of gene flow into the Batang Toru
221 population from the north than vice versa (Table S5).

222 The existence of two deep evolutionary lineages among extant Sumatran orangutans was corroborated
223 by phylogenetic analyses based on whole mitochondrial genomes (Figure 4A), in which the deepest split
224 occurred between populations north of Lake Toba and all other orangutans at ~3.97 Ma (95%-HPD:
225 2.35–5.57). Sumatran orangutans formed a paraphyletic group, with *P. tapanuliensis* being more closely
226 related to the Bornean lineage from which it diverged ~2.41 Ma (1.26–3.42 Ma). In contrast, Bornean

227 populations formed a monophyletic group with a very recent mitochondrial coalescence at ~160 ka (94–
228 227 ka).

229 Due to strong female philopatry [33], gene flow in orangutans is almost exclusively male-mediated [34].
230 Consistent with these pronounced differences in dispersal behavior, phylogenetic analysis of extensive
231 Y-chromosomal sequencing data revealed a comparatively recent coalescence of Y chromosomes of all
232 extant orangutans ~430 ka (Figure 4B). The single available Y-haplotype from *P. tapanuliensis* was
233 nested within the other Sumatran sequences, pointing at the occurrence of male-mediated gene flow
234 across the Toba divide. Thus, in combination with our modeling results, the sex-specific data highlighted
235 the impact of extraordinarily strong male-biased dispersal in the speciation process of orangutans.

236 Our analyses revealed significant divergence between *P. tapanuliensis* and *P. abelii* (Figures 3B and
237 4A), and low levels of male-mediated gene flow (Figures 3B and 4B), which, however, completely
238 ceased 10–20 ka ago (Figure 3C). Populations north and south of Lake Toba on Sumatra had been in
239 genetic contact for most of the time since their split, but there was a marked reduction in gene flow after
240 ~100 ka (Figure 3C), consistent with habitat destruction caused by the Toba supereruption 73 ka ago
241 [35]. However, *P. tapanuliensis* and *P. abelii* have been on independent evolutionary trajectories at least
242 since the late Pleistocene/early Holocene, as gene flow between these populations has ceased completely
243 10–20 ka (Figure 3C) and is now impossible because of habitat loss in areas between the species' ranges
244 [7].

245 Nowadays, most biologists would probably adopt an operational species definition such as: 'a species
246 is a population (or group of populations) with fixed heritable differences from other such populations
247 (or groups of populations)' [36]. With totally allopatric populations, a 'reproductive isolation' criterion,
248 such as is still espoused by adherents of the biological species concept, is not possible [37, 38].
249 Notwithstanding a long-running debate about the role of gene flow during speciation and genetic
250 interpretations of the species concept [39, 40], genomic studies have found evidence for many instances
251 of recent or ongoing gene flow between taxa which are recognized as distinct and well-established
252 species. This includes examples within each of the other three hominid genera. A recent genomic study
253 using comparable methods to ours revealed extensive gene flow between *Gorilla gorilla* and *G. beringei*
254 until ~20–30 ka [41]. Similar, albeit older and less extensive, admixture occurred between *Pan*
255 *troglodytes* and *P. paniscus* [42], and was also reported for *Homo sapiens* and *H. neanderthalensis* [43].
256 *Pongo tapanuliensis* and *P. abelii* appear to be further examples, showing diagnostic phenotypic and
257 other distinctions that had persisted in the past despite gene flow between them.

258 Due to the challenges involved in collecting suitable specimens for morphological and genomic analyses
259 from critically endangered great apes, our description of *P. tapanuliensis* had to rely on a single skeleton
260 and two individual genomes for our main lines of evidence. When further data will become available, a
261 more detailed picture of the morphological and genomic diversity within this species and of the

262 differences to other *Pongo* species might emerge, which may require further taxonomic revision.
263 However, is not uncommon to describe species based on a single specimen (*e.g.*, [44-46]), and
264 importantly, there were consistent differences among orangutan populations from multiple independent
265 lines of evidence, warranting the designation of a new species with the limited data at hand.

266 With a census size of fewer than 800 individuals [7], *P. tapanuliensis* is the least numerous of all great
267 ape species [47]. Its range is located around 200 km from the closest population of *P. abelii* to the north
268 (Figure 2A). A combination of small population size and geographic isolation is of particular high
269 conservation concern, as it may lead to inbreeding depression [48] and threaten population persistence
270 [49]. Highlighting this, we discovered extensive runs of homozygosity in the genomes of both *P.*
271 *tapanuliensis* individuals (Figure S3), pointing at the occurrence of recent inbreeding.

272 To ensure long-term survival of *P. tapanuliensis*, conservation measures need to be implemented
273 swiftly. Due to the rugged terrain, external threats have been primarily limited to road construction,
274 illegal clearing of forests, hunting, killings during crop conflict and trade in orangutans [7, 11]. A hydro-
275 electric development has been proposed recently in the area of highest orangutan density, which could
276 impact up to 8% of *P. tapanuliensis*' habitat. This project might lead to further genetic impoverishment
277 and inbreeding, as it would jeopardize chances of maintaining habitat corridors between the western and
278 eastern range (Figure 1A), and smaller nature reserves, all of which maintain small populations of *P.*
279 *tapanuliensis*.

Uncorrected proof
Under embargo until 02/NOV/17 12PM ET
-Do not distribute without permission-

280 **Author Contributions**

281 Conceived the study and wrote the paper: MPMG, AIN, MK, EM, MGN, CG. Edited the manuscript:
282 SW, GF, CvS, AS, TMB, DAM, TBS, TD, BG, FC, KSW, EV, PotW, PR, JB, MA, AnN. Carried out
283 statistical analyses: MPMG, AIN, MGN, AnN, CG, MdM, TD, JA, MDR, AL, MP, JPM, MK, EM, AS,
284 TMB. Provided samples, and behavioral and ecological data: MGN, MPMG, AnN, AIN, GF, JA, AL,
285 MDR, BG, EJV, KSW, IS, JP, DPF, PR, WB. Performed sequencing: MPMG, IGG, MG, CR.

286 **Acknowledgments**

287 We thank the following institutions and organizations for supporting our research: Indonesian State
288 Ministry for Research and Technology, Sabah Wildlife Department, Ministry of Environment and
289 Forestry of the Republic of Indonesia, Indonesian Institute of Sciences, Leuser International Foundation,
290 Gunung Leuser National Park, Borneo Orangutan Survival Foundation, Agisoft, NVIDIA, and the 10
291 museums where we measured the specimens. This work was financially supported by University of
292 Zurich (UZH) Forschungskredit grants FK-10 (MPMG), FK-15-103 (AIN), and FK-14-094 (TBS),
293 Swiss National Science Foundation grant 3100A-116848 (MK, CvS), Leakey Foundation (MPMG),
294 A.H. Schultz Foundation grants (MK, MPMG), UZH Research Priority Program ‘Evolution in Action’
295 (MK), the Arcus Foundation (EM), Australian National University (ANU) research fund (AnN), ANU
296 Vice Chancellor Travel Grant (AnN), Australia Awards Scholarship-DFAT (AnN), ERC Starting Grant
297 260372 (TMB), EMBO YIP 2013 (TMB), MINECO BFU2014-55090-P, BFU2015-7116-ERC,
298 BFU2015-6215-ERCU01, and MH106874 (TMB), Fundacio Zoo Barcelona (TMB), Julius-Klaus
299 Foundation (MK), MINECO/FEDER BFU2016-77961-P (JB, MP), Gates Cambridge Trust (TD), and
300 the Department of Anthropology at the University of Zurich. Novel raw sequencing data have been
301 deposited into the European Nucleotide Archive (ENA; <http://www.ebi.ac.uk/ena>) under study
302 accession number PRJEB19688.

303 **References**

- 304 1. Groves, C.P. (2001). Primate taxonomy, (Washington, D.C. ; London: Smithsonian Institution
305 Press).
- 306 2. Xu, X., and Arnason, U. (1996). The mitochondrial DNA molecule of Sumatran orangutan and
307 a molecular proposal for two (Bornean and Sumatran) species of orangutan. *J. Mol. Evol.* *43*,
308 431-437.
- 309 3. Wich, S.A., Utami Atmoko, S.S., Mitra Setia, T., and van Schaik, C.P. (2009). Orangutans:
310 geographic variation in behavioral ecology and conservation, (Oxford University Press).
- 311 4. Nederlandsch-Indische Vereeniging tot Natuurbescherming (1939). *Natuur in Zuid- en Oost-*
312 *Borneo. Fauna, flora en natuurbescherming in de Zuider- en Ooster-Afdeeling van Borneo.* In
313 *3 Jaren Indisch natuur leven. Opstellen over landschappen, dieren en planten, tevens elfde*
314 *verslag (1936-1938), Nederlandsch-Indische Vereeniging tot Natuurbescherming, ed. (Batavia,*
315 *Indonesia), pp. 334-411.*
- 316 5. Groves, C.P., Westwood, C., and Shea, B.T. (1992). Unfinished business - Mahalanobis and a
317 clockwork orang. *J. Hum. Evol.* *22*, 327-340.
- 318 6. Groves, C.P. (1986). Systematics of the great apes. In *Comparative primate biology, Vol.1:*
319 *Systematics, evolution, and anatomy*, D.R. Swindler and J. Erwin, eds. (New York: Alan R.
320 Liss), pp. 187-217.
- 321 7. Wich, S.A., Singleton, I., Nowak, M.G., Utami Atmoko, S.S., Nisam, G., Arif, S.M., Putra,
322 R.H., Ardi, R., Fredriksson, G., Usher, G., et al. (2016). Land-cover changes predict steep
323 declines for the Sumatran orangutan (*Pongo abelii*). *Sci. Adv.* *2*, e1500789.
- 324 8. Laumonier, Y., Uryu, Y., Stüwe, M., Budiman, A., Setiabudi, B., and Hadian, O. (2010). Eco-
325 floristic sectors and deforestation threats in Sumatra: identifying new conservation area network
326 priorities for ecosystem-based land use planning. *Biodivers. Conserv.* *19*, 1153-1174.
- 327 9. Wich, S.A., Usher, G., Peters, H.H., Khakim, M.F.R., Nowak, M.G., and Fredriksson, G.M.
328 (2014). Preliminary data on the highland Sumatran orangutans (*Pongo abelii*) of Batang Toru.
329 In *High Altitude Primates*, B.N. Grow, S. Gursky-Doyen and A. Krzton, eds. (New York, NY:
330 Springer New York), pp. 265-283.
- 331 10. Meijaard, E. (1997). A survey of some forested areas in South and Central Tapanuli, North
332 Sumatra; new chances for orangutan conservation. (Wageningen: Tropenbos and the Golden
333 Ark).
- 334 11. Wich, S.A., Fredriksson, G.M., Usher, G., Peters, H.H., Priatna, D., Basalamah, F., Susanto,
335 W., and Kuhl, H. (2012). Hunting of Sumatran orang-utans and its importance in determining
336 distribution and density. *Biol. Conserv.* *146*, 163-169.
- 337 12. Kramm, W. (1879). Tochtjes in Tapanoeli. *Sumatra-Courant* *20*, 1-2.
- 338 13. Miller, G.S. (1903). Mammals collected by Dr. W.L. Abbott on the coast and islands of
339 northwest Sumatra. *Proceedings US National Museum, Washington* *26*, 437-484.
- 340 14. Coolidge, H.J. (1933). *Fan Paniscus*. Pigmy chimpanzee from south of the Congo River. *Am.*
341 *J. Phys. Anthropol.* *18*, 1-59.
- 342 15. Shea, B.T., Leigh, S.R., and Groves, C.P. (1993). Multivariate craniometric variation in
343 chimpanzees. In *Species, Species Concepts and Primate Evolution*, W.H. Kimbel and L.B.
344 Martin, eds. (Boston, MA: Springer US), pp. 265-296.
- 345 16. Stumpf, R.M., Polk, J.D., Oates, J.F., Jungers, W.L., Heesy, C.P., Groves, C.P., and Fleagle,
346 J.G. (2002). Patterns of diversity in gorilla cranial morphology. In *Gorilla biology: a*
347 *multidisciplinary perspective*, A.B. Taylor and M.L. Goldsmith, eds. (Cambridge: Cambridge
348 University Press), pp. 35-61.
- 349 17. Groves, C.P. (2002). A history of gorilla taxonomy. In *Gorilla biology: a multidisciplinary*
350 *perspective*, A.B. Taylor and M.L. Goldsmith, eds. (Cambridge: Cambridge University Press),
351 pp. 15-34.
- 352 18. Geissmann, T., Lwin, N., Aung, S.S., Aung, T.N., Aung, Z.M., Hla, T.H., Grindley, M., and
353 Momberg, F. (2011). A new species of snub-nosed monkey, genus *Rhinopithecus* Milne-
354 Edwards, 1872 (Primates, Colobinae), from northern Kachin state, northeastern Myanmar. *Am.*
355 *J. Primatol.* *73*, 96-107.

- 356 19. Jones, T., Ehardt, C.L., Butynski, T.M., Davenport, T.R., Mpunga, N.E., Machaga, S.J., and De
357 Luca, D.W. (2005). The highland mangabey *Lophocebus kipunji*: a new species of African
358 monkey. *Science* 308, 1161-1164.
- 359 20. Li, C., Zhao, C., and Fan, P.F. (2015). White-cheeked macaque (*Macaca leucogenys*): a new
360 macaque species from Medog, southeastern Tibet. *Am. J. Primatol.* 77, 753-766.
- 361 21. Munds, R.A., Nekaris, K.A., and Ford, S.M. (2013). Taxonomy of the Bornean slow loris, with
362 new species *Nycticebus kayan* (Primates, Lorisidae). *Am. J. Primatol.* 75, 46-56.
- 363 22. Rasoloarison, R.M., Weisrock, D.W., Yoder, A.D., Rakotondravony, D., and Kappeler, P.M.
364 (2013). Two new species of mouse lemurs (Cheirogaleidae: *Microcebus*) from Eastern
365 Madagascar. *Int. J. Primatol.* 34, 455-469.
- 366 23. Svensson, M.S., Bersacola, E., Mills, M.S.L., Munds, R.A., Nijman, V., Perkin, A., Masters,
367 J.C., Couette, S., Nekaris, K.A.I., and Bearder, S.K. (2017). A giant among dwarfs: a new
368 species of galago (Primates: Galagidae) from Angola. *Am. J. Phys. Anthropol.* 163, 30-43.
- 369 24. Davenport, T.R.B., Stanley, W.T., Sargis, E.J., De Luca, D.W., Mpunga, N.E., Machaga, S.J.,
370 and Olson, L.E. (2006). A new genus of African monkey, *Rungwecebus*: Morphology, ecology,
371 and molecular phylogenetics. *Science* 312, 1378-1381.
- 372 25. Fan, P.F., He, K., Chen, X., Ortiz, A., Zhang, B., Zhao, C., Li, Y.Q., Zhang, H.B., Kimock, C.,
373 Wang, W.Z., et al. (2017). Description of a new species of Hoolock gibbon (Primates:
374 Hylobatidae) based on integrative taxonomy. *Am. J. Primatol.* 79.
- 375 26. Jost, L. (2008). G_{st} and its relatives do not measure differentiation. *Mol. Ecol.* 17, 4015-4026.
- 376 27. Whitlock, M.C. (2011). G_{st} and D do not replace F_{st}. *Mol. Ecol.* 20, 1083-1091.
- 377 28. Nater, A., Arora, N., Greminger, M.P., van Schaik, C.P., Singleton, I., Wich, S.A., Fredriksson,
378 G., Perwitasari-Farajallah, D., Pamungkas, J., and Krützen, M. (2013). Marked population
379 structure and recent migration in the critically endangered Sumatran orangutan (*Pongo abelii*).
380 *J. Hered.* 104, 2-13.
- 381 29. Nielsen, R., and Wakeley, J. (2001). Distinguishing migration from isolation: a Markov chain
382 Monte Carlo approach. *Genetics* 158, 885-896.
- 383 30. Palsboll, P.J., Berube, M., Aguilar, A., Notarbartolo-Di Sciara, G., and Nielsen, R. (2004).
384 Discerning between recurrent gene flow and recent divergence under a finite-site mutation
385 model applied to North Atlantic and Mediterranean Sea fin whale (*Balaenoptera physalus*)
386 populations. *Evolution* 58, 670-675.
- 387 31. Beaumont, M.A., Zhang, W.Y., and Balding, D.J. (2002). Approximate Bayesian computation
388 in population genetics. *Genetics* 162, 2025-2035.
- 389 32. Meijaard, E. (2004). Solving mammalian riddles: a reconstruction of the Tertiary and
390 Quaternary distribution of mammals and their palaeoenvironments in island South-East Asia.
391 (Australian National University), p. 2 v.
- 392 33. Arora, N., Van Noordwijk, M.A., Ackermann, C., Willems, E.P., Nater, A., Greminger, M.,
393 Nietlisbach, P., Dunkel, L.P., Utami Atmoko, S.S., Pamungkas, J., et al. (2012). Parentage-
394 based pedigree reconstruction reveals female matrilineal clusters and male-biased dispersal in
395 nongregarious Asian great apes, the Bornean orang-utans (*Pongo pygmaeus*). *Molecular*
396 *ecology* 21, 3352-3362.
- 397 34. Nater, A., Nietlisbach, P., Arora, N., van Schaik, C.P., van Noordwijk, M.A., Willems, E.P.,
398 Singleton, I., Wich, S.A., Goossens, B., Warren, K.S., et al. (2011). Sex-biased dispersal and
399 volcanic activities shaped phylogeographic patterns of extant orangutans (genus: *Pongo*). *Mol.*
400 *Biol. Evol.* 28, 2275-2288.
- 401 35. Chesner, C.A., Rose, W.I., Deino, A., Drake, R., and Westgate, J.A. (1991). Eruptive history of
402 earth's largest Quaternary caldera (Toba, Indonesia) clarified. *Geology* 19, 200-203.
- 403 36. Groves, C.P., and Grubb, P. (2011). *Ungulate taxonomy*, (Baltimore, Md.: Johns Hopkins
404 University Press).
- 405 37. Coyne, J.A., and Orr, H.A. (2004). *Speciation*, (Sunderland, MA: Sinauer Associates, Inc.).
- 406 38. Mayr, E. (1963). *Animal species and evolution*, (Cambridge,: Belknap Press of Harvard
407 University Press).
- 408 39. Arnold, M.L. (2016). *Divergence with Genetic Exchange*, (Oxford, UK: Oxford University
409 Press).
- 410 40. Reznick, D.N., and Ricklefs, R.E. (2009). Darwin's bridge between microevolution and
411 macroevolution. *Nature* 457, 837-842.

- 412 41. Scally, A., Dutheil, J.Y., Hillier, L.W., Jordan, G.E., Goodhead, I., Herrero, J., Hobolth, A.,
413 Lappalainen, T., Mailund, T., Marques-Bonet, T., et al. (2012). Insights into hominid evolution
414 from the gorilla genome sequence. *Nature* 483, 169-175.
- 415 42. de Manuel, M., Kuhlwilm, M., Frandsen, P., Sousa, V.C., Desai, T., Prado-Martinez, J.,
416 Hernandez-Rodriguez, J., Dupanloup, I., Lao, O., Hallast, P., et al. (2016). Chimpanzee genomic
417 diversity reveals ancient admixture with bonobos. *Science* 354, 477.
- 418 43. Kuhlwilm, M., Gronau, I., Hubisz, M.J., de Filippo, C., Prado-Martinez, J., Kircher, M., Fu, Q.,
419 Burbano, H.A., Lalueza-Fox, C., de la Rasilla, M., et al. (2016). Ancient gene flow from early
420 modern humans into Eastern Neanderthals. *Nature* 530, 429-433.
- 421 44. Alba, D.M., Almecija, S., DeMiguel, D., Fortuny, J., de los Rios, M.P., Pina, M., Robles, J.M.,
422 and Moya-Sola, S. (2015). Miocene small-bodied ape from Eurasia sheds light on hominoid
423 evolution. *Science* 350.
- 424 45. Stevens, N.J., Seiffert, E.R., O'Connor, P.M., Roberts, E.M., Schmitz, M.D., Krause, C.,
425 Gorscak, E., Ngasala, S., Hieronymus, T.L., and Temu, J. (2013). Palaeontological evidence for
426 an Oligocene divergence between Old World monkeys and apes. *Nature* 497, 611-614.
- 427 46. Zalmout, I.S., Sanders, W.J., MacLatchy, L.M., Gunnell, G.F., Al-Mufarreh, Y.A., Ali, M.A.,
428 Nasser, A.A.H., Al-Masari, A.M., Al-Sobhi, S.A., Nadhra, A.O., et al. (2010). New Oligocene
429 primate from Saudi Arabia and the divergence of apes and Old World monkeys. *Nature* 466,
430 360-U111.
- 431 47. IUCN (2016). IUCN Red List of Threatened Species. Version 2016.2.
- 432 48. Hedrick, P.W., and Kalinowski, S.T. (2000). Inbreeding depression in conservation biology.
433 *Annu. Rev. Ecol. Syst.* 31, 139-162.
- 434 49. Allendorf, F.W., Luikart, G., and Aitken, S.N. (2013). Conservation and the genetics of
435 populations, 2nd Edition, (Hoboken: John Wiley & Sons).
- 436 50. Locke, D.P., Hillier, L.W., Warren, W.C., Worley, K.C., Nazareth, L.V., Muzny, D.M., Yang,
437 S.-P., Wang, Z., Chinwalla, A.T., Minx, P., et al. (2011). Comparative and demographic analysis
438 of orang-utan genomes. *Nature* 469, 529-533.
- 439 51. Prado-Martinez, J., Sudmant, P.H., Kidd, J.M., Li, H., Kelley, J.L., Lorente-Galdos, B.,
440 Veeramah, K.R., Woerner, A.E., O'Connor, T.D., Santpere, G., et al. (2013). Great ape genetic
441 diversity and population history. *Nature* 499, 471-475.
- 442 52. Arora, N., Nater, A., van Schaik, C.P., Willems, E.P., van Noordwijk, M.A., Goossens, B.,
443 Morf, N., Bastian, M., Knott, C., Morrogh-Bernard, H., et al. (2010). Effects of Pleistocene
444 glaciations and rivers on the population structure of Bornean orangutans (*Pongo pygmaeus*).
445 *Proceedings of the National Academy of Sciences* 107, 21376-21381.
- 446 53. Nater, A., Nietlisbach, P., Arora, N., van Schaik, C.P., van Noordwijk, M.A., Willems, E.P.,
447 Singleton, I., Wich, S.A., Goossens, B., Warren, K.S., et al. (2011). Sex-biased dispersal and
448 volcanic activities shaped phylogeographic patterns of extant orangutans (genus: *Pongo*).
449 *Molecular Biology and Evolution* 28, 2275-2288.
- 450 54. van Noordwijk, M.A., Arora, N., Willems, E.P., Dunkel, L.P., Amda, R.N., Mardianah, N.,
451 Ackermann, C., Krützen, M., and van Schaik, C.P. (2012). Female philopatry and its social
452 benefits among Bornean orangutans. *Behavioral Ecology and Sociobiology* 66, 823-834.
- 453 55. Morrogh-Bernard, H.C., Morf, N.V., Chivers, D.J., and Krützen, M. (2011). Dispersal patterns
454 of orang-utans (*Pongo* spp.) in a Bornean peat-swamp forest. *International Journal of*
455 *Primatology* 32, 362-376.
- 456 56. Nietlisbach, P., Arora, N., Nater, A., Goossens, B., Van Schaik, C.P., and Krützen, M. (2012).
457 Heavily male-biased long-distance dispersal of orang-utans (genus: *Pongo*), as revealed by Y-
458 chromosomal and mitochondrial genetic markers. *Molecular ecology* 21, 3173-3186.
- 459 57. Nater, A., Greminger, M.P., Arora, N., van Schaik, C.P., Goossens, B., Singleton, I., Verschoor,
460 E.J., Warren, K.S., and Krützen, M. (2015). Reconstructing the demographic history of orang-
461 utans using Approximate Bayesian Computation. *Molecular Ecology* 24, 310-327.
- 462 58. Drummond, A.J., Suchard, M.A., Xie, D., and Rambaut, A. (2012). Bayesian phylogenetics
463 with BEAUti and the BEAST 1.7. *Molecular biology and evolution* 29, 1969-1973.
- 464 59. Tamura, K., and Nei, M. (1993). Estimation of the number of nucleotide substitutions in the
465 control region of mitochondrial DNA in humans and chimpanzees. *Molecular Biology and*
466 *Evolution* 10, 512-526.

- 467 60. Darriba, D., Taboada, G.L., Doallo, R., and Posada, D. (2012). jModelTest 2: more models, new
468 heuristics and parallel computing. *Nature Methods* 9, 772-772.
- 469 61. Röhrer-Ertl, O. (1988). Research history, nomenclature, and taxonomy of the orang-utan. In
470 *Orang-utan Biology*, J. Schwartz, ed. (Oxford, UK: Oxford University Press), pp. 7-18.
- 471 62. Shapiro, J.S. (1995). Morphometric variation in the orang utan (*Pongo pygmaeus*), with a
472 comparison of inter- and intraspecific variability in the African apes. Volume PhD Dissertation.
473 (Columbia University).
- 474 63. Hooijer, D.A. (1948). Prehistoric teeth of man and of the orang utan from Central Sumatra, with
475 notes on the fossil orang utan from Java and Southern China. *Zool Meded Rijksmus Leiden* 29,
476 175 - 183.
- 477 64. Drawhorn, G.M. (1994). The systematics and Paleodemography of fossil Orangutans (Genus
478 *Pongo*). (University of California).
- 479 65. Harrison, T., Jin, C., Zhang, Y., Wang, Y., and Zhu, M. (2014). Fossil *Pongo* from the Early
480 Pleistocene Gigantopithecus fauna of Chongzuo, Guangxi, southern China. *Quaternary*
481 *International* 354, 59-67.
- 482 66. de Vos, J. (1983). The *Pongo* faunas from Java and Sumatra and their significance for
483 biostratigraphical and paleo-ecological interpretations. *Proceedings of the Koninklijke*
484 *Akademie van Wetenschappen. Series B* 86, 417-425.
- 485 67. Bacon, A.-M., Westaway, K., Antoine, P.-O., Durringer, P., Blin, A., Demeter, F., Ponche, J.-
486 L., Zhao, J.-X., Barnes, L.M., Sayavonkhamdy, T., et al. (2015). Late Pleistocene mammalian
487 assemblages of Southeast Asia: New dating, mortality profiles and evolution of the predator-
488 prey relationships in an environmental context. *Palaeogeography, Palaeoclimatology,*
489 *Palaeoecology* 422, 101-127.
- 490 68. Louys, J. (2012). Mammal community structure of Sundanese fossil assemblages from the Late
491 Pleistocene, and a discussion on the ecological effects of the Toba eruption. *Quaternary*
492 *International* 258, 80-87.
- 493 69. Schwartz, J.H., Vu The, L., Nguyen Lan, C., Le Trung, K., and Tattersall, I. (1995). A review
494 of the Pleistocene hominoid fauna of the Socialist Republic of Vietnam (excluding
495 Hylobatidae).
- 496 70. Plavcan, J.M. (1994). Comparison of four simple methods for estimating sexual dimorphism in
497 fossils. *Am J Phys Anthropol* 94, 465-476.
- 498 71. Greminger, M.P., Stolting, K., Nater, A., Goossens, B., Arora, N., Bruggmann, R., Patrignani,
499 A., Nussberger, B., Sharma, R., Kraus, R.H., et al. (2014). Generation of SNP datasets for
500 orangutan population genomics using improved reduced-representation sequencing and direct
501 comparisons of SNP calling algorithms. *BMC genomics* 15, 16.
- 502 72. Andrews, S. (2012). FastQC. A quality control tool for high throughput sequence data.
- 503 73. Li, H., and Durbin, R. (2009). Fast and accurate short read alignment with Burrows-Wheeler
504 transform. *Bioinformatics* 25, 1754-1760.
- 505 74. McKenna, A., Hanna, M., Banks, E., Sivachenko, A., Cibulskis, K., Kernysky, A., Garimella,
506 K., Altshuler, D., Gabriel, S., Daly, M., et al. (2010). The Genome Analysis Toolkit: A
507 MapReduce framework for analyzing next-generation DNA sequencing data. *Genome Research*
508 20, 1297-1303.
- 509 75. DePristo, M.A., Banks, E., Poplin, R., Garimella, K.V., Maguire, J.R., Hartl, C., Philippakis,
510 A.A., del Angel, G., Rivas, M.A., Hanna, M., et al. (2011). A framework for variation discovery
511 and genotyping using next-generation DNA sequencing data. *Nat Genet* 43, 491-498.
- 512 76. Derrien, T., Estellé, J., Marco Sola, S., Knowles, D.G., Raineri, E., Guigó, R., and Ribeca, P.
513 (2012). Fast Computation and Applications of Genome Mappability. *PLoS ONE* 7, e30377.
- 514 77. Auton, A., and McVean, G. (2007). Recombination rate estimation in the presence of hotspots.
515 *Genome Research* 17, 1219-1227.
- 516 78. Auton, A., Fledel-Alon, A., Pfeifer, S., Venn, O., Segurel, L., Street, T., Leffler, E.M., Bowden,
517 R., Aneas, I., Broxholme, J., et al. (2012). A fine-scale chimpanzee genetic map from population
518 sequencing. *Science* 336, 193-198.
- 519 79. Delaneau, O., Marchini, J., and Zagury, J.F. (2012). A linear complexity phasing method for
520 thousands of genomes. *Nat Methods* 9, 179-181.
- 521 80. Delaneau, O., Howie, B., Cox, A.J., Zagury, J.F., and Marchini, J. (2013). Haplotype estimation
522 using sequencing reads. *American Journal of Human Genetics* 93, 687-696.

- 523 81. McQuillan, R., Leutenegger, A.L., Abdel-Rahman, R., Franklin, C.S., Pericic, M., Barac-Lauc,
524 L., Smolej-Narancic, N., Janicijevic, B., Polasek, O., Tenesa, A., et al. (2008). Runs of
525 homozygosity in European populations. *American Journal of Human Genetics* 83, 359-372.
- 526 82. Pemberton, Trevor J., Absher, D., Feldman, Marcus W., Myers, Richard M., Rosenberg,
527 Noah A., and Li, Jun Z. (2012). Genomic Patterns of Homozygosity in Worldwide Human
528 Populations. *The American Journal of Human Genetics* 91, 275-292.
- 529 83. Hall, T.A. (1999). BioEdit: a user-friendly biological sequence alignment editor and analysis
530 program for Windows 95/98/NT. In *Nucleic acids symposium series, Volume 41*. pp. 95-98.
- 531 84. Roos, C., Zinner, D., Kubatko, L., Schwarz, C., Yang, M., Meyer, D., Nash, S., Xing, J., Batzer,
532 M., Brameier, M., et al. (2011). Nuclear versus mitochondrial DNA: evidence for hybridization
533 in colobine monkeys. *BMC Evolutionary Biology* 11, 77.
- 534 85. Thalmann, O., Serre, D., Hofreiter, M., Lukas, D., Eriksson, J., and Vigilant, L. (2005). Nuclear
535 insertions help and hinder inference of the evolutionary history of gorilla mtDNA. *Molecular
536 Ecology* 14, 179-188.
- 537 86. Steiper, M.E., and Young, N.M. (2006). Primate molecular divergence dates. *Molecular
538 phylogenetics and evolution* 41, 384-394.
- 539 87. Bellott, D.W., Hughes, J.F., Skaletsky, H., Brown, L.G., Pyntikova, T., Cho, T.-J., Koutseva,
540 N., Zaghoul, S., Graves, T., and Rock, S. (2014). Mammalian Y chromosomes retain widely
541 expressed dosage-sensitive regulators. *Nature* 508, 494-499.
- 542 88. Soh, Y.S., Alföldi, J., Pyntikova, T., Brown, L.G., Graves, T., Minx, P.J., Fulton, R.S.,
543 Kremitzki, C., Koutseva, N., and Mueller, J.L. (2014). Sequencing the mouse Y chromosome
544 reveals convergent gene acquisition and amplification on both sex chromosomes. *Cell* 159, 800-
545 813.
- 546 89. Hughes, J.F., Skaletsky, H., Pyntikova, T., Graves, T.A., van Daalen, S.K., Minx, P.J., Fulton,
547 R.S., McGrath, S.D., Locke, D.P., and Friedman, C. (2010). Chimpanzee and human Y
548 chromosomes are remarkably divergent in structure and gene content. *Nature* 463, 536-539.
- 549 90. Wei, W., Ayub, Q., Chen, Y., McCarthy, S., Hou, Y., Carbone, I., Xue, Y., and Tyler-Smith, C.
550 (2013). A calibrated human Y-chromosomal phylogeny based on resequencing. *Genome
551 research* 23, 388-395.
- 552 91. Li, H., Handsaker, B., Wysoker, A., Fennell, T., Ruan, J., Homer, N., Marth, G., Abecasis, G.,
553 Durbin, R., and Subgroup, G.P.D.P. (2009). The Sequence Alignment/Map format and
554 SAMtools. *Bioinformatics* 25, 2078-2079.
- 555 92. Danecek, P., Auton, A., Abecasis, G., Albers, C.A., Banks, E., DePristo, M.A., Handsaker, R.E.,
556 Lunter, G., Marth, G.T., Sherry, S.T., et al. (2011). The variant call format and VCFtools.
557 *Bioinformatics* 27, 2156-2158.
- 558 93. Tavaré, S. (1986). Some probabilistic and statistical problems in the analysis of DNA sequences.
559 In *Lectures on Mathematics in the Life Sciences, Volume 17*. pp. 57-86.
- 560 94. Posada, D. (2003). Using MODELTEST and PAUP* to Select a Model of Nucleotide
561 Substitution. In *Current Protocols in Bioinformatics*. (John Wiley & Sons, Inc.).
- 562 95. Drummond, A.J., Ho, S.Y., Phillips, M.J., and Rambaut, A. (2006). Relaxed phylogenetics and
563 dating with confidence. *PLoS biology* 4, e88.
- 564 96. Yang, Z., and Rannala, B. (2006). Bayesian estimation of species divergence times under a
565 molecular clock using multiple fossil calibrations with soft bounds. *Molecular biology and
566 evolution* 23, 212-226.
- 567 97. Brunet, M., Guy, F., Pilbeam, D., Mackaye, H.T., Likius, A., Ahounta, D., Beauvilain, A.,
568 Blondel, C., Bocherens, H., and Boisserie, J.-R. (2002). A new hominid from the Upper
569 Miocene of Chad, Central Africa. *Nature* 418, 145-151.
- 570 98. Vignaud, P., Douring, P., Mackaye, H.T., Likius, A., Blondel, C., Boisserie, J.-R., De Bonis,
571 L., Eisenmann, V., Etienne, M.-E., and Geraads, D. (2002). Geology and palaeontology of the
572 Upper Miocene Toros-Menalla hominid locality, Chad. *Nature* 418, 152-155.
- 573 99. Raaum, R.L., Sterner, K.N., Noviello, C.M., Stewart, C.-B., and Disotell, T.R. (2005).
574 Catarrhine primate divergence dates estimated from complete mitochondrial genomes:
575 concordance with fossil and nuclear DNA evidence. *J Hum Evol* 48, 237-257.
- 576 100. Rambaut, A., Suchard, M.A., Xie, D., and Drummond, A.J. (2014). Tracer v1.6.
- 577 101. Rambaut, A. (2012). FigTree version 1.4.

- 578 102. Tamura, K., Stecher, G., Peterson, D., Filipski, A., and Kumar, S. (2013). MEGA6: Molecular
579 Evolutionary Genetics Analysis Version 6.0. *Molecular biology and evolution* 30, 2725-2729.
- 580 103. Scally, A., and Durbin, R. (2012). Revising the human mutation rate: implications for
581 understanding human evolution. *Nature Reviews Genetics* 13, 745-753.
- 582 104. Ségurel, L., Wyman, M.J., and Przeworski, M. (2014). Determinants of Mutation Rate Variation
583 in the Human Germline. *Annual Review of Genomics and Human Genetics* 15, 47-70.
- 584 105. Venn, O., Turner, I., Mathieson, I., de Groot, N., Bontrop, R., and McVean, G. (2014). Strong
585 male bias drives germline mutation in chimpanzees. *Science* 344, 1272-1275.
- 586 106. Lipson, M., Loh, P.-R., Sankararaman, S., Patterson, N., Berger, B., and Reich, D. (2015).
587 Calibrating the human mutation rate via ancestral recombination density in diploid genomes.
588 *PLoS Genet* 11, e1005550.
- 589 107. Carbone, L., Alan Harris, R., Gnerre, S., Veeramah, K.R., Lorente-Galdos, B., Huddleston, J.,
590 Meyer, T.J., Herrero, J., Roos, C., Aken, B., et al. (2014). Gibbon genome and the fast karyotype
591 evolution of small apes. *Nature* 513, 195-201.
- 592 108. Wich, S., De Vries, H., Ancrenaz, M., Perkins, L., Shumaker, R., Suzuki, A., and Van Schaik,
593 C. (2009). Orangutan life history variation. In *Orangutans - Geographic Variation in Behavioral
594 Ecology and Conservation* S.A. Wich, S.S. Utami Atmoko, T. Mitra Setia and C.P. van Schaik,
595 eds. (Oxford University Press), pp. 65-75.
- 596 109. Team, R.D.C. (2010). R: a language and environment for statistical computing. (Vienna,
597 Austria: R Foundation for Statistical Computing).
- 598 110. Alexander, D.H., Novembre, J., and Lange, K. (2009). Fast model-based estimation of ancestry
599 in unrelated individuals. *Genome Research* 19, 1655-1664.
- 600 111. Purcell, S., Neale, B., Todd-Brown, K., Thomas, L., Ferreira, M.A., Bender, D., Maller, J.,
601 Sklar, P., de Bakker, P.I., Daly, M.J., et al. (2007). PLINK: a tool set for whole-genome
602 association and population-based linkage analyses. *Am J Hum Genet* 81, 559-575.
- 603 112. Schiffels, S., and Durbin, R. (2014). Inferring human population size and separation history
604 from multiple genome sequences. *Nat. Genet.* 46, 919-925.
- 605 113. Robinson, J.D., Bunnefeld, L., Hearn, J., Stone, G.N., and Hickerson, M.J. (2014). ABC
606 inference of multi-population divergence with admixture from unphased population genomic
607 data. *Mol. Ecol.* 23, 4458-4471.
- 608 114. Excoffier, L., Smouse, P.E., and Quattro, J.M. (1992). Analysis of molecular variance inferred
609 from metric distances among DNA haplotypes - application to human mitochondrial DNA
610 restriction data. *Genetics* 131, 479-491.
- 611 115. Hudson, R.R. (2002). Generating samples under a Wright-Fisher neutral model of genetic
612 variation. *Bioinformatics* 18, 337-338.
- 613 116. Le Cao, K.A., Gonzalez, I., and Dejean, S. (2009). integrOmics: an R package to unravel
614 relationships between two omics datasets. *Bioinformatics* 25, 2855-2856.
- 615 117. Csillery, K., Francois, O., and Blum, M.G.B. (2012). abc: an R package for approximate
616 Bayesian computation (ABC). *Methods Ecol. Evol.* 3, 475-479.
- 617 118. Mevik, B.H. and Wehrens, R. (2007). The pls package: principal component and partial least
618 squares regression in R. *J. Stat. Softw.* 18.
- 619 119. Wegmann, D., Leuenberger, C., and Excoffier, L. (2009). Efficient Approximate Bayesian
620 computation coupled with Markov chain Monte Carlo without likelihood. *Genetics* 182, 1207-
621 1218.
- 622 120. Leuenberger, C., and Wegmann, D. (2010). Bayesian computation and model selection without
623 likelihoods. *Genetics* 184, 243-252.
- 624 121. Wegmann, D., Leuenberger, C., Neuenschwander, S., and Excoffier, L. (2010). ABCtoolbox: a
625 versatile toolkit for approximate Bayesian computations. *BMC Bioinformatics* 11.
- 626 122. Cook, S.R., Gelman, A., and Rubin, D.B. (2006). Validation of software for Bayesian models
627 using posterior quantiles. *J. Comput. Graph. Stat.* 15, 675-692.
- 628 123. Rice, W.R. (1989). Analyzing tables of statistical tests. *Evolution* 43, 223-225.
- 629 124. Gronau, I., Hubisz, M.J., Gulko, B., Danko, C.G., and Siepel, A. (2011). Bayesian inference of
630 ancient human demography from individual genome sequences. *Nat. Genet.* 43, 1031-1034.
- 631 125. Baele, G., Lemey, P., Bedford, T., Rambaut, A., Suchard, M.A., and Alekseyenko, A.V. (2012).
632 Improving the accuracy of demographic and molecular clock model comparison while
633 accommodating phylogenetic uncertainty. *Mol Biol Evol* 29, 2157-2167.

- 634 126. Raftery, A.E., Newton, M.A., Satagopan, J.M., and Krivitsky, P.N. (2007). Estimating the
635 integrated likelihood via posterior simulation using the harmonic mean identity. In Bayesian
636 Statistics, J.M. Bernardo, M.J. Bayarri and J.O. Berger, eds. (Oxford: Oxford University Press),
637 pp. 1-45.
- 638 127. Röhrer-Ertl, O. (1984). Orang-utan Studien, (Neuried, Germany: Hieronymus Verlag).
- 639 128. Röhrer-Ertl, O. (1988). Cranial growth. In Orang-utan Biology, J. Schwartz, ed. (Oxford, UK:
640 Oxford University Press), pp. 201-224.
- 641 129. Courtenay, J., Groves, C., and Andrews, P. (1988). Inter- or intra-island variation? An
642 assessment of the differences between Bornean and Sumatran orang-utans. In Orang-utan
643 biology, H. Schwartz, ed. (Oxford, England: Oxford University Press), pp. 19-29.
- 644 130. Uchida, A. (1998). Variation in tooth morphology of *Pongo pygmaeus*. *J Hum Evol* 34, 71-79.
- 645 131. Taylor, A.B. (2006). Feeding behavior, diet, and the functional consequences of jaw form in
646 orangutans, with implications for the evolution of *Pongo*. *J Hum Evol* 50, 377-393.
- 647 132. Taylor, A.B. (2009). The functional significance of variation in jaw form in orangutans. In
648 Orangutans: geographic variation in behavioral ecology and conservation, S.A. Wich, S.U.
649 Atmoko, T.M. Setia and C.P. van Schaik, eds. (Oxford, UK.: Oxford University Press), pp. 15-
650 31.
- 651 133. Tukey, J.W. (1977). Exploratory data analysis, (London, UK: Addison-Wesley Publishing
652 Company).
- 653 134. Tabachnick, B.G., and Fidell, L.S. (2013). Using multivariate statistics, 6th ed. (New York,
654 USA: Pearson).
- 655 135. R Core Development Team (2016). R: A language and environment for statistical computing.
656 R Foundation for Statistical Computing. <http://www.R-project.org/>. (Vienna, Austria).
- 657 136. Kaiser, H.F. (1960). The application of electronic computers to factor analysis. *Education and
658 Psychological Measurement* 20, 141-151.
- 659 137. Revelle, W. (2016). Psych: procedures for personality and psychological research.
660 <http://CRAN.R-project.org/package=psych> Version =1.6.4. (Evanston, Illinois, USA:
661 Northwestern University).
- 662 138. Davila-Ross, M. (2004). The long calls of wild male orangutans: A phylogenetic approach.
663 Volume PhD. (Hannover, Germany: Institut für Zoologie, Tierärztliche Hochschule Hannover).
- 664 139. Davila-Ross, M., and Geissmann, T. (2007). Call diversity of wild male orangutans: a
665 phylogenetic approach. *Am. J. Primatol.* 69, 305-324.
- 666 140. Lameira, A.R., and Wich, S.A. (2008). Orangutan Long Call Degradation and Individuality
667 Over Distance: A Playback Approach. *Int. J. Primatol.* 29, 615-625.
- 668 141. Delgado, R.A., Lameira, A.R., Davila Ross, M., Husson, S.J., Morrogh-Bernard, H.C., and
669 Wich, S.A. (2009). Geographical variation in orangutan long calls. In Orangutans: Geographic
670 variation in behavioral ecology and conservation, S.A. Wich, S.S. Utami Atmoko, T. Mitra Setia
671 and C.P. van Schaik, eds. (Oxford, UK: Oxford University Press), pp. 215-224.
- 672 142. Darul Sukma, W.P., Dai, J., Hidayat, A., Yayat, A.H., Sumulyadi, H.Y., Hendra, S., Buurman,
673 P., and Balsem, T. (1990). Explanatory booklet of the land unit and soil map of the Sidikalang
674 sheet (618), Sumatra. (Bogor, Indonesia: Centre for Soil and Agroclimate Research).
- 675 143. Darul Sukma, W.P., Suratman, Hidayat, J.A., and Budhi, P.G. (1990). Explanatory booklet of
676 the land unit and soil map of the Tapaktuan sheet (519), Sumatra, (Bogor, Indonesia: Centre for
677 Soil and Agroclimate Research).
- 678 144. Darul Sukma, W.P., Suratman, Hidayat, J.A., and Budi, P.G. (1990). Explanatory booklet of the
679 land unit and soil map of the Lho'Kruet sheet (420), Sumatra, (Bogor, Indonesia: Centre for
680 Soil and Agroclimate Research).
- 681 145. Darul Sukma, W.P., Verhagen, V., Dai, J., Buurman, P., Balsem, T., Suratman, and Vejre, H.
682 (1990). Explanatory booklet of the land unit and soil map of the Takengon sheet (520), Sumatra,
683 (Bogor, Indonesia: Centre for Soil and Agroclimate Research).
- 684 146. Hidayat, A., Verhagen, A., Darul Sukma, W.P., Buurman, P., Balsem, T., Suratman, and Vejre,
685 H. (1990). Explanatory booklet of the land unit and soil map of the Lhokseumawe (521) and
686 Simpangulim (621) sheets, Sumatra, (Centre for Soil and Agroclimate Research).
- 687 147. Hikmatullah, Wahyunto, Chendy, T.F., Dai, J., and Hidayat, A. (1990). Explanatory booklet of
688 the land unit and soil map of the Langsa (620) sheet, Sumatra, (Bogor, Indonesia: Centre for
689 Soil and Agroclimate Research).

- 690 148. Subardja, D., Djuanda, K., Hadian, Y., Samdan, C.D., Mulyadi, Y., Supriatna, W., and Dai, J.
691 (1990). Explanatory booklet of the land unit and soil map of the Sibolga (617) and
692 Padangsidempuan (717) sheets, Sumatra, (Bogor, Indonesia: Centre for Soil and Agroclimate
693 Research).
- 694 149. Wahyunto, Puksi, D.S., Rochman, A., Wahdini, W., Paidi, Dai, J., Hidayat, A., Buurman, P.,
695 and Balsem, T. (1990). Explanatory booklet of the land unit and soil map of the Medan (619)
696 sheet, Sumatra, (Bogor, Indonesia: Centre for Soil and Agroclimate Research).
- 697 150. Hall, R., van Hattum, M.W.A., and Spakman, W. (2008). Impact of India–Asia collision on SE
698 Asia: The record in Borneo. *Tectonophysics* 451, 366-389.
- 699 151. Hijmans, R.J., Cameron, S.E., Parra, J.L., Jones, P.G., and Jarvis, A. (2005). Very high
700 resolution interpolated climate surfaces for global land areas. *International Journal of*
701 *Climatology* 25, 1965-1978.
- 702 152. Wich, S.A., Singleton, I., Nowak, M.G., Utami Atmoko, S.S., Nisam, G., Arif, S.M., Putra,
703 R.H., Ardi, R., Fredriksson, G., Usher, G., et al. (2016). Land-cover changes predict steep
704 declines for the Sumatran orangutan (*Pongo abelii*). *Science Advances* 2, e1500789.
- 705 153. Wich, S.A., Atmoko, S.U., Setia, T.M., and van Schaik, C. (2009). Orangutans. *Geographic*
706 *variation in behavioral ecology and conservation*, (Oxford, UK: Oxford University Press).
- 707 154. Hall, T.A. (1999). BioEdit: a user-friendly biological sequence alignment editor and analysis
708 program for Windows 95/98/NT. *Nucleic acids symposium series* 41, 95-98.
- 709 155. Li, H., Handsaker, B., Wysoker, A., Fennell, T., Ruan, J., Homer, N., Marth, G., Abecasis, G.,
710 and Durbin, R. (2009). The sequence alignment/map format and SAMtools. *Bioinformatics* 25,
711 2078-2079.
- 712 156. Danecek, P., Auton, A., Abecasis, G., Albers, C.A., Banks, E., DePristo, M.A., Handsaker, R.E.,
713 Lunter, G., Marth, G.T., Sherry, S.T., et al. (2011). The variant call format and VCFtools.
714 *Bioinformatics* 27, 2156-2158.
- 715 157. Patterson, N., Moorjani, P., Luo, Y., Mallick, S., Rohland, N., Zhan, Y., Genschoreck, T.,
716 Webster, T., and Reich, D. (2012). Ancient admixture in human history. *Genetics* 192, 1065-
717 1093.
- 718 158. Venables, W.N., and Ripley, B.D. (2002). *Modern applied statistics with S*, 4th edition, (New
719 York, USA: Springer).

Under embargo until 02NOV2016
-Do not distribute without permission-

720 **Figure 1. Morphological evidence supporting a new orangutan species.** A) Current distribution of
 721 *Pongo tapanuliensis* on Sumatra. The holotype locality is marked with a red star. The area shown in the
 722 map is indicated in Figure 2A. B) Holotype skull and mandible of *P. tapanuliensis* from a recently
 723 deceased individual from Batang Toru. See also Figure S1, Tables S1 and S2. C) Violin plots of the
 724 first seven principal components of 26 cranio-mandibular morphological variables of 8 north Sumatran
 725 *P. abelii* and 19 Bornean *P. pygmaeus* individuals of similar developmental state as the holotype skull
 726 (black horizontal lines). See also Figure S2.

727 **Figure 2. Distribution, genomic diversity, and population structure of the genus *Pongo*.** A)
 728 Sampling areas across the current distribution of orangutans. The contour indicates the extent of the
 729 exposed Sunda Shelf during the last glacial maximum. The black rectangle delimits the area shown in
 730 Figure 1A. n = numbers of sequenced individuals. See also Table S4. B) Principal component analysis
 731 of genomic diversity in *Pongo*. Axis labels show the percentages of the total variance explained by the
 732 first two principal components. Colored bars in the insert represent the distribution of nucleotide
 733 diversity in genome-wide 1-Mb windows across sampling areas. C) Bayesian clustering analysis of
 734 population structure using the program ADMIXTURE. Each vertical bar depicts an individual, with
 735 colors representing the inferred ancestry proportions with different assumed numbers of genetic clusters
 736 (K, horizontal sections).

737 **Figure 3. Demographic history and gene flow in *Pongo*.** A) Model selection by Approximate
 738 Bayesian Computation (ABC) of plausible colonization histories of orangutans on Sundaland. The ABC
 739 analyses are based on the comparison of ~3,000 non-coding 2-kb loci randomly distributed across the
 740 genome with corresponding data simulated under the different demographic models. The numbers in
 741 the black boxes indicate the model's posterior probability. NT = Sumatran populations north of Lake
 742 Toba, ST = the Sumatran population of Batang Toru south of Lake Toba, BO = Bornean populations.
 743 B) ABC parameter estimates based on the full demographic model with colonization pattern inferred in
 744 panel A. Numbers in grey rectangles represent point estimates of effective population size (N_e). Arrows
 745 indicate gene flow among populations, numbers above the arrows represent point estimates of numbers
 746 of migrants per generation. See also Table S5. C) Relative cross-coalescent rate (RCCR) analysis for
 747 between-species pairs of phased high-coverage genomes. A RCCR close to 1 indicates extensive gene
 748 flow between species, while a ratio close to 0 indicates genetic isolation between species pairs. The x-
 749 axis shows time scaled in years, assuming a generation time of 25 years and an autosomal mutation rate
 750 of 1.5×10^{-8} per site per generation. See also Figure S3.

751 **Figure 4. Sex-specific evolutionary history of orangutans.** Bayesian phylogenetic trees for (A)
 752 mitochondrial genomes and (B) Y chromosomes. The mitochondrial tree is rooted with a human and a
 753 central chimpanzee sequence, the Y chromosome tree with a human sequence (not shown). ** Posterior
 754 probability = 1.00. C) Genotype-sharing matrix for mitogenomes (above the diagonal) and Y

755 chromosomes (below the diagonal) for all analyzed male orangutans. A value of 1 indicates that two
756 males have identical genotypes at all polymorphic sites; a value of 0 means that they have different
757 genotypes at all variable positions.

Uncorrected proof -
Under embargo until 02NOV17/12PM ET
-Do not distribute without permission-

758 CONTACT FOR RESOURCE SHARING

759 Further information and requests for resources and reagents should be directed to and will be fulfilled
760 by the Lead Contact, Michael Krützen (michael.krutzen@aim.uzh.ch).

761 EXPERIMENTAL MODEL AND SUBJECT DETAILS

762 Sample collection and population assignment for genomic analysis

763 Our sample set comprised genomes from 37 orangutans, representing the entire geographic range of
764 extant orangutans (Figure 2A). We obtained whole-genome sequencing data for the study individuals
765 from three different sources (Table S4): (i) genomes of 17 orangutans were sequenced for this study.
766 Data for 20 individuals were obtained from (ii) Locke *et al.* [50] (n=10) and (iii) Prado-Martinez *et al.*
767 [51] (n=10). All individuals were wild-born, except for five orangutans which were first-generation
768 offspring of wild-born parents of the same species (Table S4).

769 Population provenance of the previously sequenced orangutans [50, 51] was largely unknown. We
770 identified their most likely natal area based on mtDNA haplotype clustering in a phylogenetic tree
771 together with samples of known geographic provenance. Because of extreme female philopatry in
772 orangutans, mtDNA haplotypes are reliable indicators for the population of origin [33, 52-56]. Using
773 three concatenated mtDNA genes (16S ribosomal DNA, Cytochrome b, and NADH-ubiquinone
774 oxidoreductase chain 3), we constructed a Bayesian tree, including 127 non-invasively sampled wild
775 orangutans from 15 geographic regions representing all known extant orangutan populations [53, 57].
776 Gene sequences of our study individuals were extracted from their complete mitochondrial genome
777 sequences. The phylogenetic tree was built with BEAST v1.8.0. [58], as described in Nater *et al.* [53],
778 applying a TN93+I substitution model [59] as determined by jModelTest v2.1.4. [60].

779 Using the mitochondrial tree, we assigned all previously sequenced orangutans [50, 51] to their most
780 likely population of origin. Our sample assignment revealed incomplete geographic representation of
781 the genus *Pongo* in previous studies. To achieve a more complete representation of extant orangutans,
782 we sequenced genomes of 17 wild-born orangutans mainly from areas with little or no previous sample
783 coverage. Detailed provenance information for these individuals is provided in Table S4.

784 Samples for morphological analysis

785 We conducted comparative morphological analyses of 34 adult male orangutans from 10 institutions
786 housing osteological specimens. A single adult male skeleton from the Batang Toru population was
787 available for study, having died from injuries sustained in an orangutan-human conflict situation in
788 November 2013. To account for potential morphological differences related to developmental stage [61,
789 62], our analyses included only males at a similar developmental stage as the Batang Toru specimen,

790 *i.e.*, having a sagittal crest of <10 mm in height. In addition to the single available Batang Toru male,
791 our extant sample comprises specimens from the two currently recognized species, the north Sumatran
792 *Pongo abelii* (n=8) and the Bornean *P. pygmaeus* (n=25).

793 We also evaluated the relationship of the dental material between the Batang Toru specimen and those
794 of the Late Pleistocene fossil material found within the Djamboe, Lida Ajer, and Sibrambang caves near
795 Padang, Sumatra, all of which has been previously described by Hooijer [63]. Some scholars have
796 suggested that the fossil material may represent multiple species [64, 65]. However, Hooijer had more
797 than adequately shown that the variation in dental morphology observed within the three cave
798 assemblages can easily be accommodated within a single species [63]. As only teeth were present in
799 the described cave material, many of which also have gnaw marks, taphonomic processes (*e.g.*,
800 porcupines as accumulating agents) are thought to have largely shaped the cave material [66, 67] and
801 thus may account for the appearance of size differences among the cave samples [64, 65]. Furthermore,
802 the similarities in the reconstructed age of the cave material (~128-118 ka or ~80-60 ka [66-68]), and
803 the fact that the presence of more than one large-bodied ape species is an uncommon feature in both
804 fossil and extant Southeast Asian faunal assemblages [69], makes it highly unlikely that multiple large-
805 bodied ape species co-existed within the area at a given time. For purposes of discussion here, we
806 collectively refer to the Padang fossil material as *P. p. palaeosumatrensis*, as described by Hooijer [63].

807 As the comparative fossil sample likely comprises various age-sex classes [63], we divided the fossil
808 sample into two portions above and below the mean for each respective tooth utilized in this study. We
809 considered samples above the mean to represent larger individuals, which we attribute to “males”, and
810 the ones below to being smaller individuals, which we attribute to “females” [70]. We only used the
811 “male” samples in comparison to our extant male comparative orangutan sample.

812 **METHOD DETAILS**

813 **Whole-genome sequencing**

814 To obtain sufficient amounts of DNA, we collected blood samples from confiscated orangutans at
815 rehabilitation centres, including the Sumatran Orangutan Conservation Program (SOCP) in Medan,
816 BOS Wanariset Orangutan Reintroduction Project in East Kalimantan, Semongok Wildlife
817 Rehabilitation Centre in Sarawak, and Sepilok Orangutan Rehabilitation Centre in Sabah. We took
818 whole blood samples during routine veterinary examinations and stored in EDTA blood collection tubes
819 at -20°C. The collection and transport of samples were conducted in strict accordance with Indonesian,
820 Malaysian and international regulations. Samples were transferred to Zurich under the Convention on
821 International Trade of Endangered Species in Fauna and Flora (CITES) permit numbers 4872/2010
822 (Sabah), and 06968/IV/SATS-LN/2005 (Indonesia).

823 We extracted genomic DNA using the Genra Puregene Blood Kit (Qiagen) but modified the protocol
824 for clotted blood as described in Greminger *et al.* [71]. We sequenced individuals on two to three lanes
825 on an Illumina HiSeq 2000 in paired end (2 x 101 bp) mode. Sample PP_5062 was sequenced at the
826 Functional Genomics Center in Zurich (Switzerland), the other individuals at the Centre Nacional
827 d'Anàlisi Genòmica in Barcelona (Spain), as the individuals of Prado-Martinez *et al.* [51]. On average,
828 we generated $\sim 1.1 \times 10^9$ raw Illumina reads per individual.

829 **Read mapping**

830 We followed identical bioinformatical procedures for all 37 study individuals, using the same software
831 versions. We quality-checked raw Illumina sequencing reads with FastQC v0.10.1. [72] and mapped to
832 the orangutan reference genome *ponAbe2* [50] using the Burrows-Wheeler Aligner (BWA-MEM)
833 v0.7.5 [73] in paired-end mode with default read alignment penalty scores. We used Picard v1.101
834 (<http://picard.sourceforge.net/>) to add read groups, convert sequence alignment/map (SAM) files to
835 binary alignment/map (BAM) files, merge BAM files for each individual, and to mark optical and PCR
836 duplicates. We filtered out duplicated reads, bad read mates, reads with mapping quality zero, and reads
837 that mapped ambiguously.

838 We performed local realignment around indels and empirical base quality score recalibration (BQSR)
839 with the Genome Analysis Toolkit (GATK) v3.2.2. [74, 75]. The BQSR process empirically calculates
840 more accurate base quality scores (*i.e.*, Phred-scaled probability of error) than those emitted by the
841 sequencing machines through analysing the covariation among several characteristics of a base (*e.g.*,
842 position within the read, sequencing cycle, previous base, etc.) and its status of matching the reference
843 sequence or not. To account for true sequence variation in the data set, the model requires a database of
844 known polymorphic sites ('known sites') which are skipped over in the recalibration algorithm. Since
845 no suitable set of 'known sites' was available for the complete genus *Pongo*, we preliminary identified

846 confident SNPs from our data. For this, we performed an initial round of SNP calling on unrecalibrated
847 BAM files with the *UnifiedGenotyper* of the GATK. Single nucleotide polymorphisms were called
848 separately for Bornean and Sumatran orangutans in multi-sample mode (*i.e.*, joint analysis of all
849 individuals per island), creating two variant call (VCF) files. In addition, we produced a third VCF file
850 jointly analysing all study individuals in order to capture genus-wide low frequency alleles. We applied
851 the following hard quality filter criteria on all three VCF files: $QUAL < 50.0 \parallel QD < 2.0 \parallel FS > 60.0 \parallel$
852 $MQ < 40.0 \parallel HaplotypeScore > 13.0 \parallel MappingQualityRankSum < -12.5 \parallel ReadPosRankSum < -8.0$.
853 Additionally, we calculated the mean and standard deviation of sequencing depth over all samples and
854 filtered all sites with a site-wise coverage more than five standard deviations above the mean. We
855 merged the three hard filtered VCF files and took SNPs as ‘known sites’ for BQSR with the GATK.
856 The walkers *CountReads* and *DepthOfCoverage* of the GATK were used to obtain various mapping
857 statistics for unfiltered and filtered BAM files.

858 Mean effective sequencing depth, estimated from filtered BAM files, varied among individuals ranging
859 from 4.8–12.2x [50] to 13.7–31.1x (this study) [51], with an average depth of 18.4x over all individuals
860 (Tables S4). For the previously sequenced genomes [50, 51], estimated sequence depths were 25–40%
861 lower as the values reported in the two source studies. This difference is explained by the way sequence
862 depth was calculated. Here, we estimated sequence depth on the filtered BAM files where duplicated
863 reads, bad read mates, reads with mapping quality zero, and reads which mapped ambiguously had
864 already been removed. Thus, our sequence coverage estimates correspond to the effective read-depths
865 which are available for SNP discovery and genotyping.

866 **SNP and genotype calling**

867 We produced high quality genotypes for all individuals for each position in the genome, applying the
868 same filtering criteria for SNP and non-polymorphic positions. We identified SNPs and called
869 genotypes in a three-step approach. First, we identified a set of candidate (raw) SNPs among all study
870 individuals. Second, we performed variant quality score recalibration (VQSR) on the candidate SNPs
871 to identify high-confidence SNPs. Third, we called genotypes of all study individuals at these high-
872 confidence SNP positions.

873 Step 1: We used the *HaplotypeCaller* of the GATK in genomic Variant Call Format (gVCF) mode to
874 obtain for each individual in the dataset genotype likelihoods at any site in the reference genome.
875 *HaplotypeCaller* performs local realignment of reads around potential variant sites and is therefore
876 expected to considerably improve SNP calling in difficult-to-align regions of the genome. We then
877 genotyped the resulting gVCF files together on a per-island level, as well as combined for all
878 individuals, using the *GenotypeGVCFs* tool of the GATK to obtain three VCF files with candidate
879 SNPs for *P. abelii*, *P. pygmaeus*, and over all *Pongo* samples.

880 Step 2: Of the produced set of candidate SNPs, we identified high-confidence SNPs using the VQSR
881 procedure implemented in the GATK. The principle of the method is to develop an estimate of the
882 relationship between various SNP call annotations (*e.g.*, total depth, mapping quality, strand bias, etc.)
883 and the probability that a SNP is a true genetic variant. The model is determined adaptively based on a
884 set of ‘true SNPs’ (*i.e.*, known variants) provided as input. Our ‘true SNPs’ set contained 5,600 high-
885 confidence SNPs, which were independently identified by three different variant callers in a previous
886 reduced-representation sequencing project [71]. We ran the *Variant Recalibrator* of the GATK
887 separately for each of the three raw SNP VCFs to produce recalibration files based on the ‘true SNPs’
888 and a VQSR training set of SNPs. The VQSR training sets were derived separately for each of the three
889 raw SNP VCF files and contained the top 20% SNPs with highest variant quality score after having
890 applied hard quality filtering as described for the VCF files in the BQSR procedure.

891 We used the produced VQSR recalibration files to filter the three candidate SNP VCFs with the Apply
892 Recalibration walker of the GATK setting the ‘--truth_sensitivity_filter_level’ to 99.8%. Finally, we
893 combined all SNPs of the three VCF files passing this filter using the *Combine Variants* tool of the
894 GATK, hence generating a master list of high-confidence SNP sites in the genus *Pongo*.

895 Step 3: We called the genotype of each study individual at the identified high-confidence SNP sites.
896 We performed genotyping on the recalibrated BAM files in multi-sample mode for Bornean and
897 Sumatran orangutans separately, producing one SNP VCF file per island.

898 Finally, we only retained positions with high genome mappability, *i.e.*, genomic positions within a
899 uniquely mappable 100-mers (up to 4 mismatches allowed), as identified with the GEM-mappability
900 module from the GEM library build [76]. This mappability mask excludes genomic regions in the
901 orangutan reference genome that are duplicated and therefore tend to produce ambiguous mappings,
902 which can lead to unreliable genotype calling. Furthermore, we aimed to reduce spurious male
903 heterozygous genotype calls on the X chromosome due to *UnifiedGenotyper* assuming diploidy of the
904 entire genome. We determined the male-to-female ratios (M/F) of mean observed heterozygosity (H_o)
905 and sequence coverage in non-overlapping 20-kb windows along the X chromosome across both
906 islands. We obtained a list of X-chromosomal windows where M/F of H_o was above the 85%-quantile
907 or M/F coverage was above the 95%-quantile, resulting in 1255 20-kb windows requiring exclusion.
908 We then repeated step 3 of the genotype calling pipeline on the X chromosome for the male samples
909 setting the argument ‘-ploidy’ of *UnifiedGenotyper* to 1 to specify the correct hemizygous state of the
910 X chromosome in males. We subsequently masked all X-chromosomal positions within the spurious
911 20-kb windows in both male and female samples.

912 In total, we discovered 30,640,634 SNPs among all 37 individuals, which represent the most
913 comprehensive catalogue of genetic diversity across the genus *Pongo* to date.

914 **QUANTIFICATION AND STATISTICAL ANALYSIS**915 **Recombination map estimation**

916 We generated recombination maps for Bornean and Sumatran orangutans using the LDhat v2.2a
917 software [77], following Auton et al. [78]. We used a high-quality subset of genotype data from the
918 original SNP-calling dataset for the recombination map estimation for each island separately. Only
919 biallelic, non-missing and polymorphic SNPs were used. Filtered genotype data were split into windows
920 of 5,000 SNPs with an overlap of 100 SNPs at each side.

921 We ran the program *Interval* of the LDhat package for 60 million iterations, using a block penalty of 5,
922 with the first 20 million iterations discarded as a burn-in. A sample was taken from the MCMC chain
923 every 40,000 iterations, and a point estimate of the recombination rate between each SNP was obtained
924 as the mean across samples. We joined the rate estimates for each window at the midpoint of the
925 overlapping regions and estimated *theta per site* for each window using the finite-site version of the
926 Watterson's estimate, as described in Auton & McVean [77].

927 We tested the robustness of the method with regards to the observed genome-wide variation of *theta* by
928 contrasting recombination rate estimates using window-specific and chromosomal-average *thetas*.
929 *Thetas* twice as large that the genome average produced very similar $4N_e\mu$ (*rho*) estimates. Because of
930 this, a single genome-wide average of *theta per site* was used for all the windows (Sumatra: $\theta_w =$
931 0.001917, Borneo: $\theta_w = 0.001309$). We then applied additional filters following Auton et al. [78]. SNP
932 intervals larger than 50 kb, or *rho* estimates larger than 100, were set to zero and the 100 surrounding
933 SNP intervals (-/+ 50 intervals) were set to zero recombination rate. A total of 1,000 SNP intervals were
934 found to have $\rho > 100$ for *P. abelii*, and 703 for *P. pygmaeus*. In addition, 32 gaps (> 50 kb) were
935 identified for *P. abelii*, and 47 gaps for *P. pygmaeus*. After applying the +/- 50 interval criteria, a total
936 of 7,424 SNP intervals were zeroed for *P. abelii*, and 15,694 for *P. pygmaeus*.

937 **Haplotype phasing**

938 We phased the genotype data from Bornean and Sumatran orangutans using a read aware statistical
939 phasing approach implemented in SHAPEIT v2.0 [79, 80]. This allowed us to obtain good phasing
940 accuracy despite our relatively low sample sizes by using phasing information contained in the paired-
941 end sequencing reads to support the statistical phasing procedure. We used a high-quality subset of
942 genotype data from the original SNP-calling dataset containing only biallelic and polymorphic SNPs.
943 We first ran the program extractPIRs to extract phase informative reads (PIR) from the filtered BAM
944 files. In a second step, we ran SHAPEIT in read aware phasing mode using the following parameters:
945 200 conditional states, 10 burnin iterations, 10 pruning iterations, 50 main iterations, and a window
946 size of 0.5 Mb. Additionally, we provided two species-specific recombination maps (estimated with
947 LDhat) and the PIR files obtained in the first step to the program.

948 SHAPEIT uses a recombination map expressed in cM/Mb, therefore it was necessary to convert the
949 LDhat-based ρ estimates to cM/Mb units ($\rho=4N_e r$). Accordingly, we estimated island-specific
950 effective population sizes using the Watterson's estimator of θ (Sumatra: $N_e[\theta_w]=41,000$, Borneo:
951 $N_e[\theta_w]=27,000$) and applied these to the recombination map conversion. The most likely pair of
952 haplotypes for each individual were retrieved from the haplotype graphs, and recoded into VCF file
953 format.

954 **Individual heterozygosity and inbreeding**

955 We determined the extent of inbreeding for each individual by a genome-wide heterozygosity scan in
956 sliding windows of 1 Mb, using a step size of 200 kb. We detected an excess of windows with very low
957 heterozygosity in the density plots, pointing to some extent of recent inbreeding. To estimate the cutoff
958 values of heterozygosity for the calculation of inbreeding coefficients, we calculated heterozygosity
959 thresholds for each island according to the 5th-percentile of the genome-wide distribution of
960 heterozygosities (Borneo: 1.0×10^{-4} heterozygote sites per bp; Sumatra: 1.3×10^{-4}). Neighboring regions
961 with heterozygosities below the cutoff value were merged to determine the extent of runs of
962 homozygosity (ROH). Based on the number and size of ROHs, we estimated the percentage of the
963 genome that is autozygous, which is a good measure of inbreeding [81]. We choose 1 Mb as window
964 size for the calculation of heterozygosities based on previous studies identifying regions smaller than
965 0.5 Mb as the result of background relatedness, and tracts larger than 1.6 Mb as evidence of recent
966 parental relatedness [82].

967 **Sex-specific genomic data: mitogenomes and Y chromosomes**

968 We produced complete mitochondrial genome (mitogenome) sequences for all study individuals. We
969 first created a consensus reference sequence from 13 Sanger-sequenced mitogenomes representing
970 almost all major genetic clusters of extant orangutans using BioEdit v7.2.0. [83]. The Sanger-sequenced
971 mitogenomes were generated via 19 PCRs with product sizes of 1.0–1.2 kb and an overlap of 100–300
972 bp (Table S6) following described methods [84]. PCR conditions for all amplifications were identical
973 and comprised a pre-denaturation step at 94°C for 2 minutes, followed by 40 cycles each with
974 denaturation at 94°C for 1 minute, annealing at 52°C for 1 minute, and extension at 72°C for 1.5
975 minutes. At the end, we added a final extension step at 72°C for 5 minutes. PCR products were checked
976 on 1% agarose gels, excised from the gel and after purification with the Qiagen Gel Extraction Kit,
977 sequenced on an ABI 3130xL sequencer using the BigDye Terminator Cycle Sequencing kit (Applied
978 Biosystems) in both directions using the amplification primers.

979 We individually mapped Illumina whole-genome sequencing reads of all 37 study individuals (Table
980 S4) to the consensus mitochondrial reference sequence using NovoAlign v3.02. (NovoCraft), which
981 can accurately handle reference sequences with ambiguous bases. This procedure prevented biased

982 short read mapping due to common population-specific mutations. For each individual, we generated a
983 FASTA sequence for the mitogenome with the *mpileup* pipeline of SAMtools. We only considered
984 bases with both mapping and base Phred quality scores ≥ 30 and required all positions to be covered
985 between 100 and 2000 times. Finally, we visually checked the sequence alignment of all individuals in
986 BioEdit and manually removed indels and poorly aligned positions and excluded the D-loop to account
987 for sequencing and alignment errors in those regions which might inflate estimates of mtDNA diversity.
988 In total, we identified 1,512 SNPs among all 50 individuals.

989 We thoroughly investigated the literature for the potential occurrence of nuclear insertions of mtDNA
990 (numts) in the genus *Pongo*, given that this has been a concern in closely related gorillas (*Gorilla* spp.)
991 [85]. There was no indication of numts in the genus *Pongo*, which is in line with our own previous
992 observations [28, 52, 53]. Numts also seem unlikely given our high minimal sequence depth threshold.

993 We developed a comprehensive bioinformatics strategy to extract sequences from the male-specific
994 region of the Y chromosome (MSY) from whole-genome sequencing data. We expect the principle of
995 our bioinformatics strategy to be applicable to mammalian species in general if the taxon under
996 investigation is in phylogenetic proximity to one for which a Y-chromosomal reference sequence is
997 present or will be made available. Like most mammals, there is currently no reference Y
998 chromosome for orangutans. Therefore, we had to rely on a reference assembly of a related species (*i.e.*,
999 humans) for sequence read mapping. Despite the ~ 18 million years divergence between humans (*Homo*
1000 spp.) and orangutans [51, 86], we obtained a high number of MSY sequences. The impact of varying Y
1001 chromosome structure among species [87, 88] on sequence read mappability might have been reduced
1002 because we exclusively targeted X-degenerate regions. Hughes et al. [89] showed for human and
1003 chimpanzees that although less than 50% of ampliconic sequences have a homologous counterpart in
1004 the other species, over 90% of the X-degenerate sequences hold such a counterpart.

1005 We applied several filters to ensure male-specificity and single-copy status of the generated MSY
1006 sequences. (i) We simultaneously mapped sequencing reads to the whole orangutan reference genome
1007 *PonAbe2* [50] and not just the human reference Y chromosome, reducing spurious mapping of
1008 autosomal reads to the Y chromosome and allowing subsequent identification of reads that also aligned
1009 to the X or autosomal chromosomes. (ii) We exclusively accepted reads that mapped in a proper pair,
1010 *i.e.*, where both read mates mapped to the Y chromosome, which considerably increased confidence in
1011 Y-specific mapping. (iii) We also mapped whole-genome sequencing reads of 23 orangutan females to
1012 the human Y reference chromosome and excluded all reference positions where female reads had
1013 mapped from the male Y sequence data. (iv) To exclude potential repetitive regions, we filtered non-
1014 uniquely mapped reads as well as positions with sequence coverage greater than two times the median
1015 coverage for each individual, as extensive coverage can be indicative for repetitive regions which might
1016 appear as collapsed regions on the Y reference chromosome. (v) To ensure that we only targeted unique,

1017 single-copy MSY regions, we exclusively retained reads mapping to four well-established X-degenerate
1018 regions of the MSY in humans [90].

1019 Our bioinformatics strategy consisted of the following detailed steps. First, we created a new reference
1020 sequence (*PonAbe2_humanY*) by manually adding the human reference Y chromosome (*GRCh37*) to
1021 the orangutan reference genome *PonAbe2* [50]. We then used BWA-MEM v0.7.5. [73] to map Illumina
1022 whole-genome short reads from 36 orangutans (13 males and 23 females) to this new reference
1023 sequence. We mapped reads for each individual separately in paired-end mode and with default settings.
1024 To reduce output file size, we removed unmapped reads on the fly using SAMtools v0.1.19 [91]. Picard
1025 v1.101 was used to add read groups and sort the BAM files. We then extracted all reads which mapped
1026 to the Y chromosome using SAMtools and marked read duplicates with Picard.

1027 We used the GATK [74, 75] to perform local realignment around indels and filtered out duplicated
1028 reads, bad read mates, reads with mapping quality zero and reads which mapped ambiguously. We
1029 called genotypes at all sequenced sites with the *Unified Genotyper* of the GATK, applying the output
1030 mode 'EMIT_ALL_CONFIDENT_SITES'. We called genotypes in multi-sample mode (females and
1031 males separately, sample-ploidy was set to 1), producing one genomic VCF file for each sex. We only
1032 accepted bases/reads for genotype calling if they had Phred quality scores ≥ 30 .

1033 From the VCF file of the females, we generated a 'nonspec' list with the coordinates of all sites with
1034 coverage in more than one female (minimal sequence depth $2x$), as these sites most likely were located
1035 in pseudoautosomal or ampliconic regions, *i.e.*, share similarity with the X or autosomal chromosomes.
1036 To ensure Y-specificity, we removed all sites of the 'nonspec' list from the VCF file of the males with
1037 VCFtools v0.1.12b. [92]

1038 Finally, we used GATK to extract sequences of four well-established X-degenerate regions of the MSY
1039 in humans (14,170,438–15,795,786; 16,470,614–17,686,473; 18,837,846–19,267,356; 21,332,221–
1040 21,916,158 on the human reference Y chromosome assembly GRCh37/hg19)[90]. To be conservative,
1041 we chose regions which were longer than 1 Mb in humans and disregarded the first and last 300 kb of
1042 each region to account for potential uncertainties regarding region boundaries, leaving us with
1043 3,854,654 bp in total. We exclusively retained genotype calls that were covered by a minimum of two
1044 reads and had a maximum of twice the individual mean coverage, resulting in 2,825,271 bp of MSY
1045 sequences among the 13 orangutan males. As expected, individual mean MSY sequence depth was
1046 about half (average: 54.4%) of that recorded for the autosomes, and ranged from 2.79–16.62x. For
1047 analyses, we only kept sites without missing data, *i.e.*, with a genotype in all study males. Because
1048 genomes of some individuals had been sequenced to only low coverage (~ 5 – $7x$) [50], this left us with
1049 673,165 bp of MSY sequences. We identified 1,317 SNPs among the 13 males, corresponding to a SNP
1050 density of 1 SNP every 511 bp.

1051 We constructed phylogenetic trees and estimated divergence dates for mitogenome and MSY sequences
1052 using the Bayesian Markov chain Monte Carlo (MCMC) method implemented in BEAST v1.8.0. [58].
1053 To determine the most suitable nucleotide substitution model, we conducted model selection with
1054 jModelTest v2.1.4. [60]. Based on the Akaike information criterion (AIC) and corrected AIC, we
1055 selected the GTR+I substitution model [93] for mitogenomes and the TVM+I+G model [94] for MSY
1056 sequences.

1057 The mitogenome tree was rooted with a human and a central chimpanzee sequence from GenBank
1058 (accession numbers: GQ983109.1 and HN068590.1), the MSY tree with the human reference sequence
1059 *hg19*. We estimated divergence dates under a relaxed molecular clock model with uncorrelated
1060 lognormally distributed branch-specific substitution rates [95]. The prior distribution of node ages was
1061 generated under a birth-death speciation process [96]. We used fossil based divergence estimates to
1062 calibrate the molecular clock by defining a normal prior distribution for certain node ages. For
1063 mitogenomes, we applied two calibration points, *i.e.*, the *Pan-Homo* divergence with a mean age of 6.5
1064 Ma and a standard deviation of 0.3 Ma [97, 98] and the Ponginae-Homininae divergence with a mean
1065 age of 18.3 Ma and a larger standard deviation of 3.0 Ma [86], which accounts for the uncertainty in
1066 the divergence date [99]. For MSY sequences, we used the Ponginae-Homininae divergence for
1067 calibration. We performed four independent BEAST runs for 30 million generations each for
1068 mitogenomes, with parameter sampling every 1,000 generations, and for 200 million generations each
1069 with parameter sampling every 2,000 generations for MSY sequences. We used Tracer v1.6 [100] to
1070 examine run convergence, aiming for an effective sample size of at least 1000 for all parameters. We
1071 discarded the first 20% of samples as burn-in and combined the remaining samples of each run with
1072 LogCombiner v1.8.0. [58]. Maximum clade credibility trees were drawn with TreeAnnotator v1.8.0.
1073 [58] and trees visualized in FigTree v1.4.0. [101] and MEGA v6.06. [102].

1074 **Autosomal genetic diversity and population structure**

1075 For all subsequent population genetic analyses, we assumed an autosomal mutation rate (μ) of 1.5×10^{-8}
1076 per base pair per generation, based on estimates obtained for the present-day mutation rates in humans
1077 and chimpanzees, derived primarily from de novo sequencing comparisons of parent-offspring trios but
1078 also other evidence [103-106]. There is good reason to believe that the mutation rate in orangutans is
1079 similar to that in other great apes, given the very similar branch lengths from outgroups such as gibbon
1080 and macaque to each species [107]. We assumed a generation time of 25 years [108].

1081 We identified patterns of population structure in the autosomal genome by principal component analysis
1082 (PCA) of biallelic SNPs using the function ‘prcomp’ in R v3.2.2 [109]. Three separate analyses were
1083 performed: one within each island and one including all study individuals. For each sample set, we
1084 excluded all genotypes from the SNP VCF files that were covered by less than five reads and only
1085 retained SNPs with a genotype call in all individuals after this filter. Furthermore, we removed SNPs

1086 with more than two alleles and monomorphic SNPs in the particular sample set. This restrictive filtering
1087 left us with 3,006,895 SNPs for the analysis of all study individuals, 5,838,796 SNPs for PCA within
1088 Bornean orangutans and 4,808,077 SNPs for PCA within Sumatran orangutans.

1089 We inferred individual ancestries of orangutans using ADMIXTURE v1.23 [110]. We randomly
1090 sampled one million sites from the original VCF files and filtered this subset by excluding sites with
1091 missing genotypes or with a minor allele frequency less than 0.05. We further reduced the number of
1092 sites to 272,907 by applying a linkage disequilibrium (LD) pruning filter using PLINK v1.90b3q (`-`
1093 `indep-pairwise 50 5 0.5`) [111]. ADMIXTURE was run 20 times at all K values between 1 and 10.
1094 Among those runs with a difference to the lowest observed cross validation (CV) error of less than 0.1
1095 units, we reported the replicate with the highest biological meaning, *i.e.*, runs that resolved substructure
1096 among different sampling areas rather than identifying clusters within sampling areas.

1097 For subsequent analyses, we defined seven distinct populations based on the results of the PCA and
1098 ADMIXTURE analyses: three on Sumatra (Northeast Alas comprising North Aceh and Langkat
1099 regions, West Alas, and Batang Toru) and four on Borneo (East Kalimantan, Sarawak, Kinabatangan
1100 comprising North and South Kinabatangan, and Central/West Kalimantan comprising Central and West
1101 Kalimantan). Even though individuals from North and South Kinabatangan could be clearly
1102 distinguished in the PCA and ADMIXTURE analysis, we decided to pool the two Kinabatangan
1103 populations due to their low samples sizes ($n = 2$). This can be justified as data from the mitochondrial
1104 genome showed that they started to diverge only recently (~ 40 ka).

1105 **Ancestral gene flow between orangutan populations**

1106 We used D-statistics to assess gene flow between orangutan species, testing all three possible
1107 phylogenetic relationships among *P. abelii*, *P. tapanuliensis*, and *P. pygmaeus*. We extracted genotype
1108 data from the two individuals per population with the highest sequencing coverage and included two
1109 human genome sequences as outgroup (SRA sample accession: ERS007255 and ERS007266). We
1110 calculated D-statistics for all combinations of populations involving the three species using the qpDstat
1111 program of the ADMIXTOOLS package v4.1 and assessed significance using the block jackknife
1112 procedure implemented in ADMIXTOOLS.

1113 To explore temporal patterns of gene flow between orangutan populations, we applied the multiple
1114 sequential Markovian coalescent (MSMC2) model [112]. The rate of coalescence of between-
1115 population haplotype pairs was compared to the within-population coalescence rate of haplotype pairs
1116 from the same population to obtain the relative cross-coalescence rate (RCCR) through time. A RCCR
1117 close to 1 indicates extensive gene flow between populations, while a ratio close to 0 indicates complete
1118 genetic isolation.

1119 We used the phased whole-genome data for the relative cross-coalescence rate analysis. To avoid
1120 coverage-related issues, we selected the individual with the highest sequencing coverage for each
1121 population. We further excluded sites with an individual sequencing coverage less than 5x, a mean
1122 mapping quality less than 20, or sites with low mappability based on the mappability mask.

1123 We ran MSMC2 for all pairs of populations, using a single individual (*i.e.*, two haplotypes) per
1124 population. For each population pair, we performed three individual MSMC2 runs, using the default
1125 time discretization parameters: within population 1 (two haplotypes; -I 0,1), within population 2 (two
1126 haplotypes; -I 2,3), and between populations (four haplotypes; -I 0,1,2,3 -P 0,0,1,1). We then used the
1127 combineCrossCoal.py Python script of the MSMC2 package to combine the outputs of the three runs
1128 into a combined output file.

1129 As the sequencing coverage of the best Batang Toru individual was substantially lower compared to
1130 individuals from other populations (~17x vs. ~23–27x, Table S4), we also assessed whether different
1131 sequencing coverage was negatively affecting the relative cross-coalescence rate results. To achieve
1132 this, we repeated the analysis using individuals with similar coverage as the Batang Toru individual
1133 (~16–21x). The results were highly consistent with the output from the runs with the highest-coverage
1134 individuals, indicating that the relative cross-coalescent rate analysis was robust to differences in
1135 sequencing coverage in our data set.

1136 **Approximate Bayesian Computation (ABC)**

1137 To gain insights into the colonization history of the Sundaland region by orangutans and obtain
1138 parameter estimates of key aspects of their demographic history, we applied a model-based ABC
1139 framework [31]. For this, we sampled a total of 3,000 independent sequence loci of 2 kb each, following
1140 the recommendations in Robinson et al. [113]. Loci were sampled randomly from non-coding regions
1141 of the genome, with a minimum distance of 50 kb between loci to minimize the effects of linkage. Since
1142 the coalescent simulations underlying ABC inference assume neutrality, we excluded loci located
1143 within 10 kb of any exonic region defined in the *Pongo abelii* Ensembl gene annotation release 78, as
1144 well as loci on the X chromosome and the mitochondrial genome, which would exhibit reduced N_e as
1145 compared to the autosomal regions.

1146 For all ABC-based modelling, we defined three metapopulations for the calculation of summary
1147 statistics: Sumatran populations north of Lake Toba (NT), the Sumatran population of Batang Toru
1148 south of Lake Toba (ST), as well as all Bornean populations (BO). For each metapopulation as well as
1149 over all metapopulations combined, we calculated the first four moments over all loci for the following
1150 summary statistics: nucleotide diversity (π), Watterson's theta, and Tajima's D. Furthermore, for each
1151 of the three pairwise comparisons between metapopulations, we calculated the first four moments over
1152 loci of the number of segregating sites, proportions of shared and fixed polymorphism, average
1153 sequence divergence (d_{XY}), and Φ_{ST} [114]. To avoid potential problems with unreliable phasing, we

1154 only used summary statistics that do not require phased sequence data. This resulted in a total of 108
1155 summary statistics used in the ABC analyses. For each locus, we extracted genotype data of a total of
1156 22 individuals (5 Northeast Alas, 5 West Alas, 2 Batang Toru, 4 Central/West Kalimantan, 2 East
1157 Kalimantan, 2 Sarawak, 2 Kinabatangan) by selecting the individuals with the highest sequence
1158 coverage for a given locus. Additionally, we recorded the positions of missing data for each locus and
1159 individual and coded genotypes as ‘missing’ in the simulated data if mutations fell within the range of
1160 missing data in the observed data.

1161 In a first step, we used a model testing framework to infer the most likely sequence of population splits
1162 in the colonization history of orangutans. For this, we designed four models representing potential
1163 colonization patterns into Sundaland (Figure 3A). We assumed a simplified population structure with
1164 three distinct, random mating units composed of NT, ST, and BO metapopulations as described above.
1165 We simulated 4×10^6 data sets for each model using the coalescent simulator ms [115]. Since we obtained
1166 a large number of summary statistics, we used a partial least squares discriminant analysis (PLS-DA)
1167 to extract the orthogonal components of the summary statistics that are most informative to discriminate
1168 between the four competing models using the ‘plsda’ function of the R package ‘mixOmics’ v5.2.0
1169 [116] in R version 3.2.2 [109]. For model testing, we used the R package ‘abc’ v2.1 [117] to perform a
1170 multinomial logistic regression on the PLS transformed simulated and observed summary statistics,
1171 using a tolerance level of 0.05% (8,000 simulations closest to the observed data). To find the optimal
1172 number of PLS components for model selection, we performed cross-validations with 200 randomly
1173 chosen sets of summary statistics for each model and assessed model misspecification rates when using
1174 10, 12, 15, 18, and 20 components.

1175 We found that using the first 18 PLS components resulted in the lowest model misspecification rate.
1176 However, our model testing approach lacked power to reliably differentiate between pairs of models
1177 with the same underlying species tree (*i.e.*, model 1a vs. model 1b and model 2a vs. model 2b in Figure
1178 3A), as evidenced by a high model misspecification rate of 47.63% across all four models. In order to
1179 increase discrimination power with a new set of optimized PLS components, we therefore repeated the
1180 PLS-DA and multinomial logistic regression with the two best-fitting models (model 1a vs. model 1b).
1181 This resulted in a substantially lower model misspecification rate (36.00%). Moreover, no model
1182 misassignment occurred with a posterior probability equal or higher than the observed value (0.976),
1183 indicating a high confidence in the selected model (model 1a).

1184 After establishing the order of population split events, we were interested in parameter estimates of
1185 different aspects of the orangutan demographic history. For this, we applied a more complex model that
1186 included additional population structure in NT and BO, as well as recent population size changes
1187 (Figure 3B). The design of this model was informed by (i) PCA and ADMIXTURE analyses (Figures
1188 2B and 2C), (ii) MSMC2 analyses (Figure 3C), and (iii) previous demographic modeling using more
1189 limited sets of genetic markers [57]. For parameter estimation, we performed a total of 1×10^8 simulations

1190 as described above. Model parameterization and parameter prior distributions are shown in Table S5.
1191 We used 100,000 random simulations to extract the orthogonal components of the summary statistics
1192 that maximize the covariance matrix between summary statistics and model parameters using the ‘plsr’
1193 function of the R package ‘pls’ v2.5-0 [118]. We defined the optimal number of partial least squares
1194 (PLS) components based on the drop in the root mean squared error for each parameter with the
1195 inclusion of additional PLS components [119]. After transforming both the simulated and observed
1196 summary statistics with the loadings of the extracted PLS components, we performed ABC-GLM post-
1197 sampling regression [120] on the simulations with the smallest Euclidean distance to the observed
1198 summary statistics using ABCtoolbox v2.0 [121]. To find the optimal proportion of retained
1199 simulations, we assessed the root-mean-integrated-squared error of the parameter posterior distributions
1200 based on 1,000 pseudo-observed data sets (pods) randomly chosen from the simulated data. We found
1201 that varying the tolerance level had little impact on the accuracy of the posterior distributions and
1202 therefore used a tolerance level of 0.00002 (equaling 2,000 simulations) for parameter estimation.

1203 To assess the goodness of fit of our demographic model, we calculated the marginal density and the
1204 probability of the observed data under the general linear model (GLM) used for the post-sampling
1205 regression with ABCtoolbox [120]. A low probability of the observed data under the GLM indicates
1206 that the observed data is unlikely to have been generated under the inferred GLM, implying a bad model
1207 fit. We obtained a p-value of 0.14, showing that our complex demographic model is well able to
1208 reproduce the observed data. Additionally, we visualized the coverage of summary statistics generated
1209 under the demographic model relative to the observed data by plotting the first 12 principal components
1210 of the simulated and observed data. For this, we randomly selected 100,000 simulations and extracted
1211 PCA components using the ‘prcomp’ function in R. The observed data fell well within the range of
1212 simulated summary statistics for all 12 components. Furthermore, we checked for biased posterior
1213 distributions by producing 1,000 pods with parameter values drawn from the prior distributions. For
1214 each pods, we determined the quantile of the estimated posterior distribution within which the true
1215 parameter values fell and used a Kolmogorov-Smirnov in R to test the resulting distribution of posterior
1216 quantiles for uniformity. Deviations from uniformity indicate biased posterior distributions [122] and
1217 the corresponding parameter estimates should be treated with caution. As expected from complex
1218 demographic models, multiple parameters showed significant deviations from uniformity after
1219 sequential Bonferroni correction [123]. However, in most of these distributions, data points were
1220 overrepresented in the center of the histogram, which indicates that posterior distributions were
1221 estimated too conservatively.

1222 **G-PhoCS analysis**

1223 We used the full-likelihood approach implemented in G-PhoCS v1.2.3 [124] to compare different
1224 models of population splitting with gene flow and to estimate parameters of the best-fitting model. Due
1225 to computational constraints, we limited our data set to eight individuals with good geographic coverage
1226 of the extant orangutan distribution (1 Northeast Alas, 1 West Alas, 2 Batang Toru, 2 Central/West
1227 Kalimantan, 1 East Kalimantan, 1 Kinabatangan). We sampled 1-kb loci across the autosomal genome,
1228 ensuring a minimum distance of 50 kb among loci to minimize linkage. To reduce the impact of natural
1229 selection, we excluded loci located within 1 kb of any exonic region defined in the *Pongo abelii*
1230 Ensembl gene annotation release 78. We coded sites as missing based on the following filter criteria:
1231 low mappability, mean mapping quality less than 20, and individual coverage less than 5x. Sites without
1232 at least one valid genotype per species were excluded completely. We only retained loci with at least
1233 700 bp of sites with data, resulting in a total of 23,380 loci for which we extracted genotype information
1234 for the eight selected individuals.

1235 We compared models with the three different possible underlying population trees in a three taxon
1236 setting (Borneo, Sumatra north of Lake Toba, and Batang Toru). We performed 16 independent G-
1237 PhoCS runs for each model, running the MCMC algorithm for 300,000 iterations, discarding the first
1238 100,000 iterations as burn-in and sampling every 11th iteration thereafter. The first 10,000 iterations
1239 were used to automatically adjust the MCMC finetune parameters, aiming for an acceptance rate of the
1240 MCMC algorithm of 30–40%. We merged the resulting output files of independent runs and analysed
1241 them with Tracer v1.6 [100] to ensure convergence among runs. We then used the model comparison
1242 based on the Akaike information criterion through MCMC (AICM) [125, 126] implemented in Tracer
1243 to assess the relative fit of the three competing models.

1244 In agreement with the ABC analyses, the model positing the deepest split between Sumatra north of
1245 Lake Toba and Batang Toru, followed by a split between south of Lake Toba and Borneo, showed a
1246 much better fit to the data compared to the two other splitting patterns. Independent replicates of the
1247 same model produced highly consistent posterior distributions, indicating convergence of the MCMC
1248 algorithm. All parameters of the best-fitting model were estimated with high precision, as shown by the
1249 small 95%-highest posterior density ranges (Table S5). Compared to the estimates from the ABC
1250 analysis, G-PhoCS resulted in more recent divergence time estimates for both the NT/(BO,ST) and
1251 BO/ST splits. This discrepancy might be caused by hypermutable CpG sites, which likely violate certain
1252 assumptions of the G-PhoCS model [124]. We could not exclude CpG sites in our analysis due to the
1253 absence of a suitable outgroup for calibration. Instead, we had to rely on a fixed genome-wide mutation
1254 rate, which includes hypervariable CpG sites. An alternative explanation could be a likely bias in the
1255 G-PhoCS results due to the restriction to a highly simplified demographic model as compared to our
1256 ABC analyses; G-PhoCS assumes constant effective population sizes and migration rates in between

1257 population splits. However, this assumption is most likely violated in orangutans, as shown by the
1258 results of our ABC analysis (Figure 3B, Table S5).

1259 **Cranial, dental, and mandibular morphology**

1260 We evaluated five qualitative and 44 quantitative cranial, dental, and mandibular variables (Tables S1
1261 and S2). We chose variables that had previously been used to describe and differentiate orangutan
1262 cranio-mandibular shape [61-63, 127-132]. Due to extensive dental wear of the Batang Toru specimen,
1263 we limited our comparisons with the Padang cave material to the breadth of the upper and lower canines,
1264 in addition to the length, breadth, and area (*i.e.*, breadth x length) of the lower first molar, all of which
1265 displayed a limited amount of wear. All measurements were taken by a single individual (AnN) in order
1266 to reduce observer bias.

1267 We used both univariate and multivariate statistics to evaluate the Batang Toru specimen in relation to
1268 our comparative sample. As Batang Toru is only represented by a single sample, we first compared it
1269 to the interquartile range (IQR, defined as the range between the first and the third quartile) and the
1270 lower and upper inner fence ($\pm 1.5 \cdot \text{IQR}$) for each separate sample population, using traditional methods
1271 for evaluating outliers [133]. This allowed us to evaluate the Batang Toru specimen's distance and
1272 direction from the central tendency of our sample orangutan populations. We also conducted univariate
1273 exact permutation tests for each morphological variable by removing a single sample for either the *P.*
1274 *abelii*, *P. pygmaeus*, or *P. p. palaeosumatrensis* sample populations and then comparing the linear
1275 distance to the mean of the remaining samples. This was done for each sample until all samples had a
1276 calculated value. A linear distance between the *P. tapanuliensis* sample and the *P. abelii*, *P. pygmaeus*,
1277 and *P. p. palaeosumatrensis* mean values (*i.e.*, the test statistics) was then calculated and compared to
1278 the sample distributions detailed above. P-values represent the number of samples from the sample
1279 distribution that exceed the test statistic, divided by the total number of comparisons. In some cases,
1280 specimens did not preserve the measurements utilized in this study (*e.g.*, broken bone elements and/or
1281 missing/heavily worn teeth), and so were excluded from comparisons. Sample sizes for univariate
1282 comparisons of extant orangutan cranio-mandibular morphology are detailed in Table S1, whereas the
1283 sample sizes for the univariate comparisons of extant and fossil teeth are detailed in Table S2.

1284 We also conducted a PCA on 26 of our 39 cranio-mandibular variables, on a subset of our extant
1285 orangutan sample, including *P. abelii* (n=8), *P. pygmaeus* (n=19), and the newly described *P.*
1286 *tapanuliensis* specimen. The choice of 26 variables allowed us to maximize sample size and avoid
1287 violating the assumptions of PCA [134]. A scree plot (using the *princomp* function from the base *stats*
1288 package in R [135]) indicated that seven principal components were sufficient to be extracted, based on
1289 the Kaiser criterion of eigenvalues at ≥ 1 [136]. Using the *principal* function from the *psych* R package
1290 [137], we ran a PCA on the correlation matrix of our 26 selected variables, extracting seven principal
1291 components with varimax rotation.

1292 To highlight the multivariate uniqueness of *P. tapanuliensis*, we used the extracted PCs and calculated
1293 the Euclidean D^2 distance for each sample relative to the *P. abelii* and *P. pygmaeus* centroids. We
1294 grouped these distances into two distributions, referred to as the between species (*i.e.*, the distances of
1295 all *P. abelii* samples to the *P. pygmaeus* centroid plus all of the *P. pygmaeus* samples to the *P. abelii*
1296 centroid) and within species (*i.e.*, the distances of all *P. abelii* samples to the *P. abelii* centroid plus all
1297 of the *P. pygmaeus* samples to the *P. pygmaeus* centroid) distributions. We then compared the Euclidean
1298 D^2 distances of *P. tapanuliensis* to the *P. abelii* and *P. pygmaeus* centroids (*i.e.*, the test values), relative
1299 to the two aforementioned sample distributions. Exact permutation p-values for these results were
1300 calculated as the number of samples from the sample distribution that exceed the test statistic, divided
1301 by the total number of comparisons. All Euclidean D^2 distance were calculated in the base *stats* package
1302 in R [135].

1303 **Acoustic and behavioral analyses**

1304 We used both previously published [138-140] and newly collected data in our analyses of male long
1305 calls. The current study includes $n=130$ calls from $n=45$ adult males across 13 orangutan field sites. In
1306 addition to two individuals from Batang Toru, we sampled 14 individuals of *P. abelii* and 29 individuals
1307 of *P. pygmaeus*. Using our comparative sample, we evaluated 15 long call variables (Table S3). We
1308 chose variables and their definitions that had previously been described to differentiate orangutan male
1309 long calls [138, 139, 141].

1310 We used both univariate and multivariate statistics to evaluate the Batang Toru specimen in relation to
1311 our comparative sample. As Batang Toru is only represented by two individuals, we compared the mean
1312 of these two sample points to the interquartile range (IQR) and the lower and upper inner fence
1313 ($\pm 1.5 \times \text{IQR}$) for each separate sample population [133]. As above, univariate exact permutation tests
1314 were conducted for each long call variable by removing a single sample for either the *P. abelii* or *P.*
1315 *pygmaeus* sample populations and then comparing the linear distance to the mean of the remaining
1316 samples. This was done for each sample until all samples had a calculated value. A linear distance
1317 between the average of the two *P. tapanuliensis* samples and the *P. abelii* or *P. pygmaeus* mean values
1318 (*i.e.*, the test statistics) was then calculated and compared to the sample distributions detailed above. P-
1319 values represent the number of samples from the sample distribution that exceed the test statistic,
1320 divided by the total number of comparisons. In some cases, not all acoustic variables were available for
1321 each individual. As such, sample sizes for univariate comparisons are detailed in Table S3.

1322

1323 **Geological and ecological analyses**

1324 We evaluated five ecological variables, including the type and age of geological parent material,
1325 elevation, average temperature, and average rainfall, to highlight that the current ecological niche of *P.*

1326 *tapanuliensis* is divergent relative to that of *P. abelii* and *P. pygmaeus*. For Sumatran populations, type
1327 and age of geological parent material were digitized from the land unit and soil map series of Sumatra
1328 [142-149]. No comparable geospatial data is available for Borneo, so we used previously published
1329 materials to more broadly characterize areas populated by orangutans [150]. To maintain consistency,
1330 elevation, average temperature, and average annual rainfall were collected from the WorldClim v. 1.4
1331 bioclimatic variables dataset [151]. Using the digitized land unit/soil maps, we calculated the percentage
1332 of Sumatran orangutan distribution [152] classified into four classes for each type (*e.g.*, igneous,
1333 metamorphic, sedimentary, and other rock [*i.e.*, land units with a mixture of rock types]) and age (*e.g.*,
1334 Pre-Cenozoic, Tertiary, Quaternary, and other [*i.e.*, land units with a mixture of ages]) of geological
1335 parent material. For the elevation and climatic variables, we created 1km x 1km sample point grids for
1336 each currently identified orangutan population in Borneo and Sumatra [152, 153], and sampled the three
1337 aforementioned WorldClim datasets.

1338 **DATA AND SOFTWARE AVAILABILITY**

1339 Raw sequence read data have been deposited into the European Nucleotide Archive (ENA;
1340 <http://www.ebi.ac.uk/ena>) under study accession number PRJEB19688. Mitochondrial and Y-
1341 chromosomal sequences are available from the Mendeley Data repository under ID code
1342 doi:10.17632/hv2r94yz5n.1.

Uncorrected proof -
Under embargo until 02/10/2021
-Do not distribute without permission-

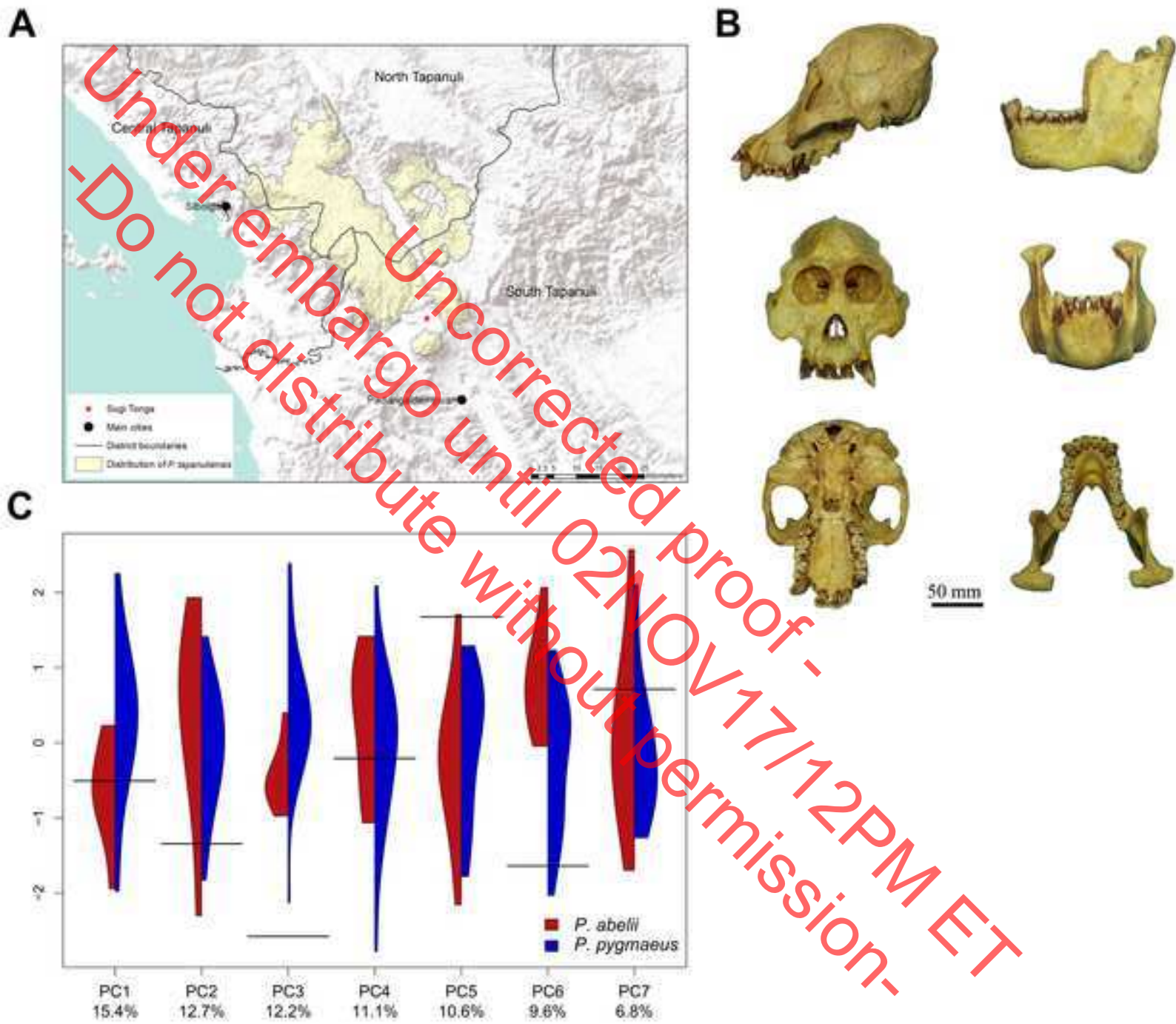
KEY RESOURCES TABLE

REAGENT or RESOURCE	SOURCE	IDENTIFIER
Biological Samples		
17 <i>Pongo</i> spp. whole blood samples	This paper	See Table S4
34 <i>Pongo</i> spp. cranial specimens	This paper	N/A
Chemicals, Peptides, and Recombinant Proteins		
Proteinase K (20 mg/ml)	Promega	Cat#V3021
Critical Commercial Assays		
Genra Puregene Blood Kit	Qiagen	Cat#158467
Deposited Data		
<i>Pongo abelii</i> reference genome <i>ponAbe2</i>	[50]	http://genome.wustl.edu/genomes/detail/pongo-abelii/
<i>Pongo abelii</i> Ensembl gene annotation release 78	Ensembl	https://www.ensembl.org/Pongo_abelii/Info/Index
Human reference genome NCBI build 37, GRCh37	Genome Reference Consortium	http://www.ncbi.nlm.nih.gov/projects/genome/assembly/grc/human/
Whole-genome sequencing data of 5 <i>Pongo abelii</i>	[50]	SRA: PRJNA20869
Whole-genome sequencing data of 5 <i>Pongo pygmaeus</i>	[50]	SRA: PRJNA74653
Whole-genome sequencing data of 10 <i>Pongo</i> spp.	[51]	SRA: PRJNA189439
Whole-genome sequencing data of 17 <i>Pongo</i> spp.	This paper	ENA: PRJEB19688
Whole-genome sequencing data of 2 <i>Homo sapiens</i>	Human Genome Diversity Project	SRA: ERS007255 and ERS007266
13 <i>Pongo</i> MSY sequences	This paper	http://dx.doi.org/10.17632/hv2r94yz5n.1
50 <i>Pongo</i> mitochondrial genome sequences	This paper	http://dx.doi.org/10.17632/hv2r94yz5n.1
Pictures of paratypes	This paper	https://morphobank.org/index.php/Projects/ProjectOverview/project_id/2591
Additional supporting information and analyses	This paper	https://morphobank.org/index.php/Projects/ProjectOverview/project_id/2591
Oligonucleotides		
19 mitochondrial primer pairs	This paper	See Table S6
Software and Algorithms		
FastQC v0.10.1.	[72]	https://www.bioinformatics.babraham.ac.uk/projects/fastqc/
BWA v0.7.5	[73]	http://bio-bwa.sourceforge.net/
Picard Tools v1.101		http://broadinstitute.github.io/picard/

GATK v3.2.2.	[74, 75]	https://software.broadinstitute.org/gatk/
GEM library	[76]	http://algorithms.wtf/gem-library
LDhat v2.2a	[77]	https://github.com/auton1/LDhat
SHAPEIT v2.0	[79]	https://mathgen.stats.ox.ac.uk/genetics_software/shapeit/shapeit.html
BioEdit v7.2.0.	[154]	http://www.mbio.ncsu.edu/bioedit/page2.htm
NovoAlign v3.02.	Novocraft	http://www.novocraft.com/products/novoalign/
SAMtools v0.1.19	[155]	http://www.htslib.org/
VCFTools v0.1.12b.	[156]	https://vcftools.github.io/index.html
BEAST v1.8.0.	[58]	http://beast.community/index.html
jModelTest v2.1.4.	[60]	https://github.com/ddarriba/jmodeltest2
Tracer v1.6		http://tree.bio.ed.ac.uk/software/tracer/
FigTree v1.4.0.		http://tree.bio.ed.ac.uk/software/figtree/
MEGA v6.06.	[102]	http://www.megasoftware.net/mega.php
R 3.2.2	[109]	https://www.r-project.org
ADMIXTURE v1.23	[110]	https://www.genetics.ucla.edu/software/admixture/index.html
PLINK v1.90b3q	[111]	https://www.cog-genomics.org/plink2
ADMIXTOOLS v4.1	[157]	https://github.com/DReichLab/AdmixTools
MSMC2	[112]	https://github.com/stschiff/msmc2
ms	[115]	http://home.uchicago.edu/rhudson1/source/mksamples.html
R package 'mixOmics' v5.2.0	[116]	https://www.rdocumentation.org/packages/mixOmics
R package 'abc' v2.1	[117]	https://cran.r-project.org/package=abc
R package 'pls' v2.5-0	[118]	https://cran.r-project.org/package=pls

ABCtoolbox v2.0	[121]	http://www.unifr.ch/biology/research/wegmann/wegmannsoft
G-PhoCS v1.2.3	[124]	http://compgen.cshl.edu/GPhoCS/
R package 'psych'	[137]	https://cran.r-project.org/package=psych
R package 'MASS'	[158]	https://cran.r-project.org/package=MASS

Uncorrected proof -
Under embargo until 02NOV17/12PM ET
-Do not distribute without permission-



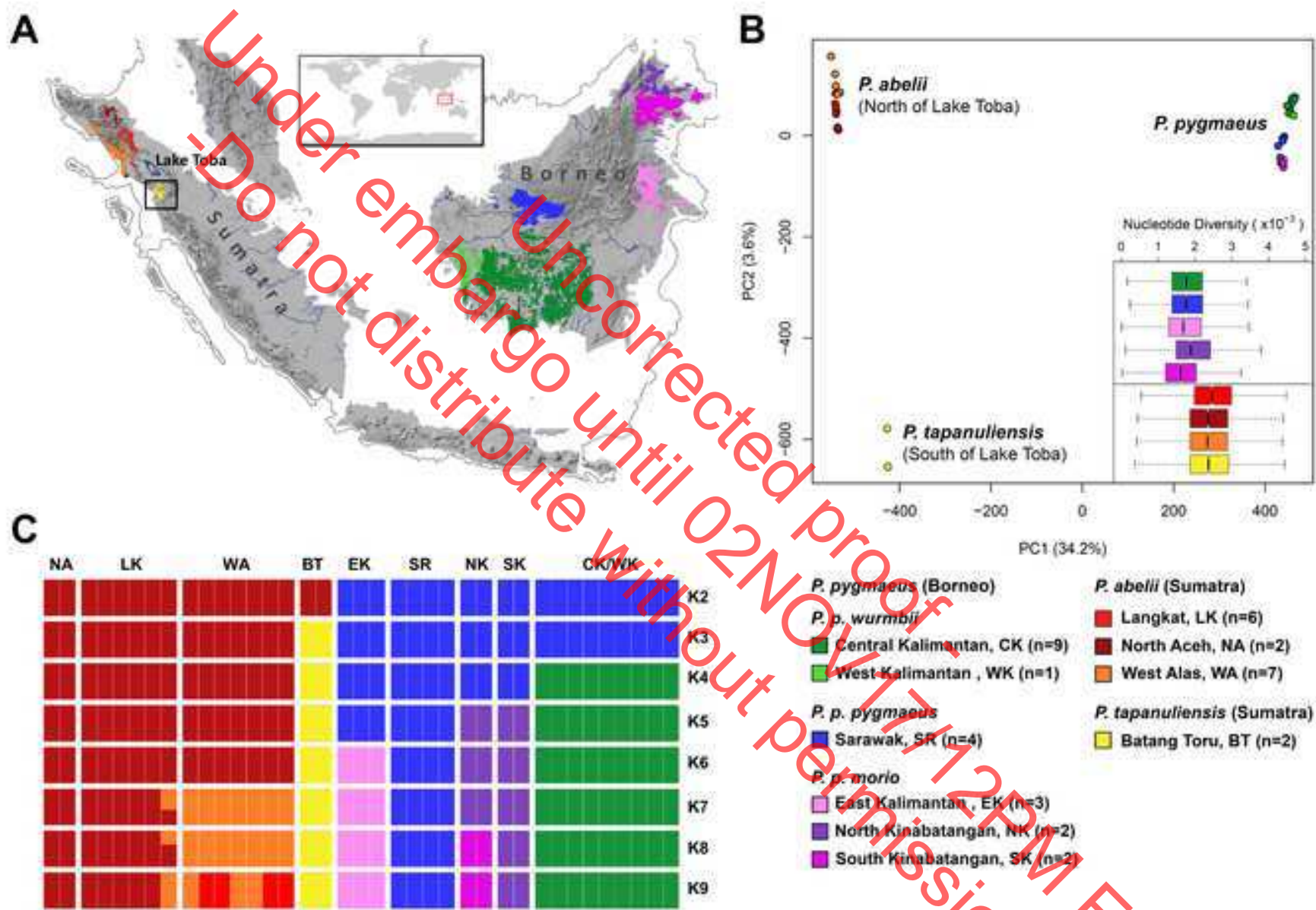
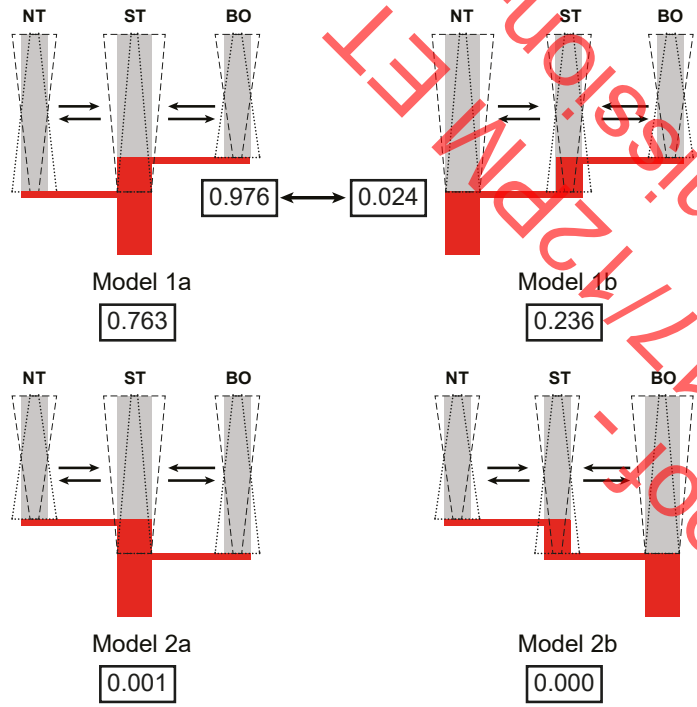
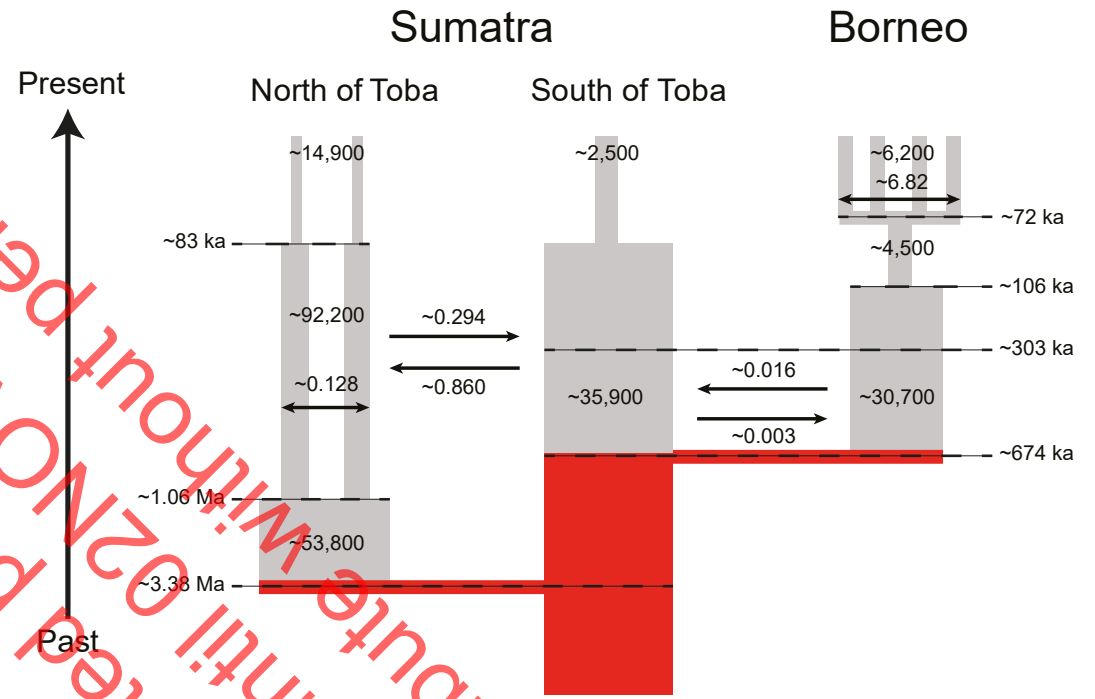


Figure 3

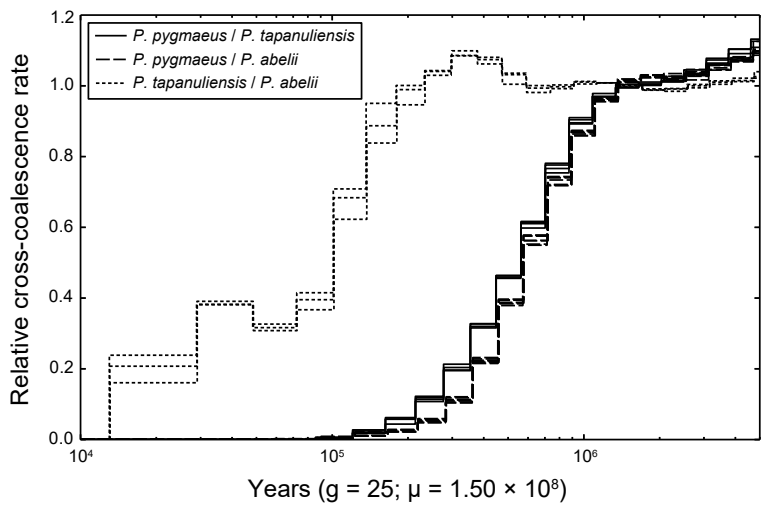
A



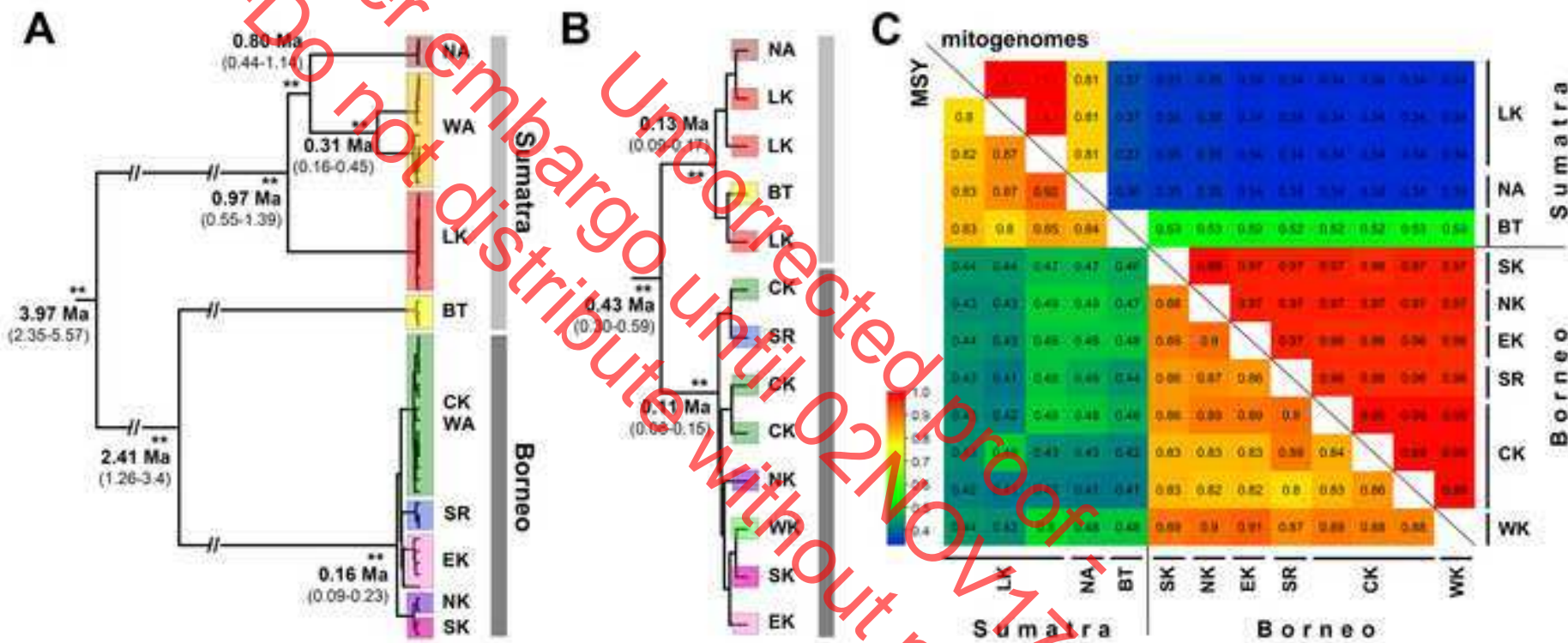
B



C



Uncorrected proof - Do not distribute without permission until 02 NOV 17 12 PM ET



Under embargo until 02 NOV 17 / 12PM ET
 -Do not distribute without permission-

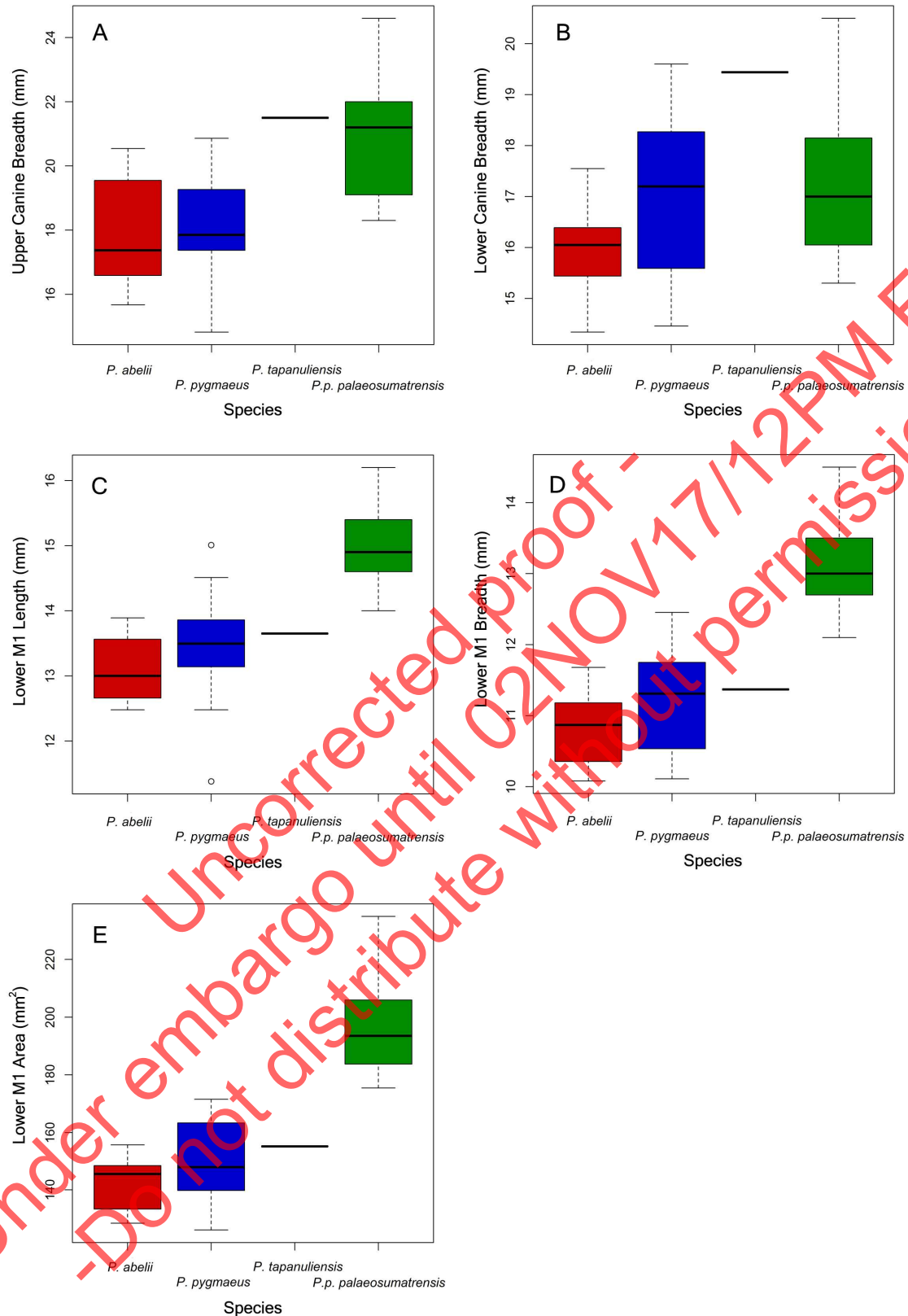


Figure S1. Comparisons of five dental variables across *P. abelii* (red), *P. pygmaeus* (blue), *P. tapanuliensis* (black horizontal line), and *P. p. palaeosumatrensis* (green). Related to Figure 1B. Variables include upper canine breadth (A), lower canine breadth (B), lower M1 length (C), lower M1

breadth (D), and lower M1 area (E). For each boxplot, the middle line is the median value of the distribution, with the box representing the first (lower extreme) and third (upper extreme) quartile values (*i.e.*, the interquartile range [IQR]), and the whiskers representing the lower and upper extreme values that are within 1.5 x IQR of the first and third quartile values. Exact permutation analyses suggested that *P. tapanuliensis* could be differentiated statistically from the *P. abelii* mean for both the upper (p-value<0.001) and lower canine breadths (p-value<0.001) and from the *P. 'pygmaeus' palaeosumatrensis* mean for lower M₁ length (p-value<0.001), breadth (p-value<0.001), and area (p-value<0.001). *P. tapanuliensis* could not be differentiated statistically from the *P. pygmaeus* mean for any of the five dental measures.

Uncorrected proof -
Under embargo until 02NOV17/12PM ET
-Do not distribute without permission-

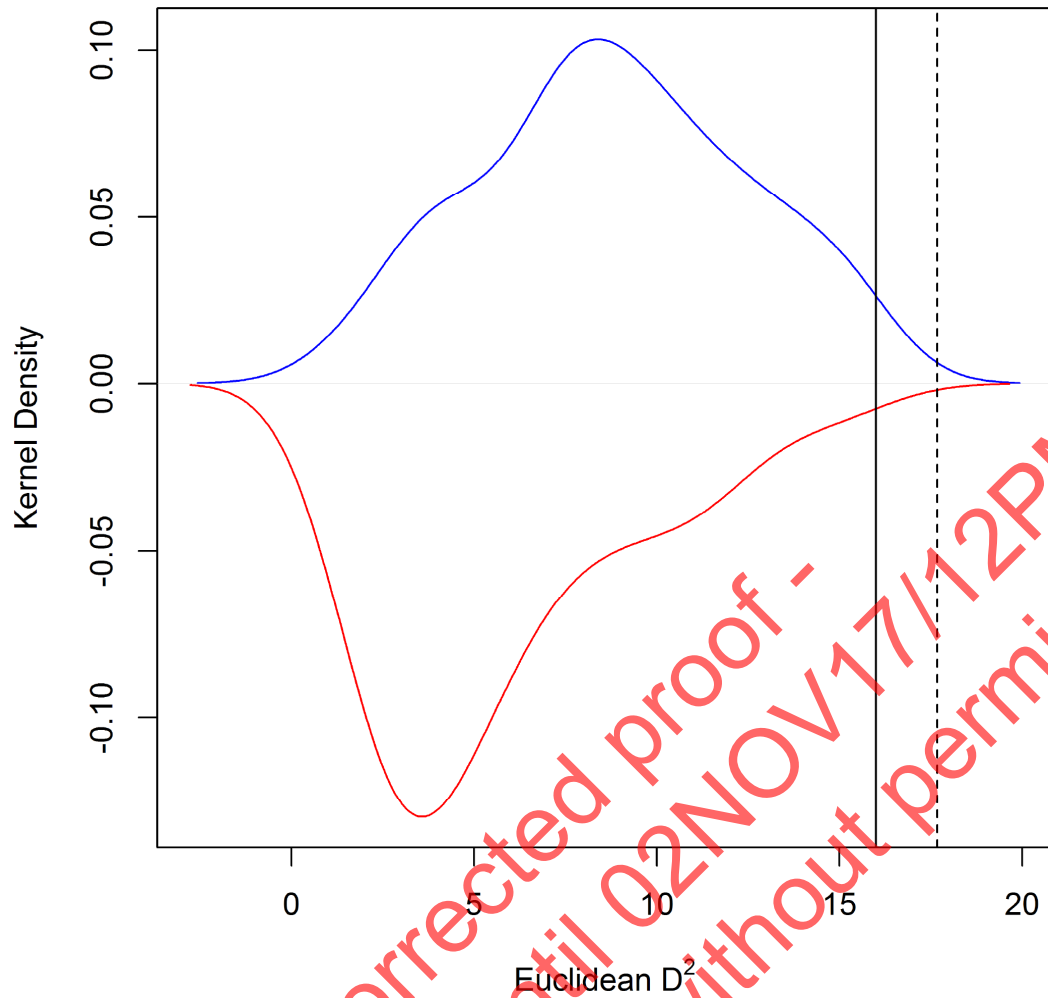


Figure S2. Kernel density mirror plot of Euclidean D^2 analyses of six principal components calculated from 26 cranio-mandibular morphological variables. Related to Figure 1C. The between-species distribution (blue line) was calculated as the distances of all *P. abelii* samples to the *P. pygmaeus* centroid plus all of the *P. pygmaeus* samples to the *P. abelii* centroid, whereas the within-species distribution (red line) was calculated as the distances of all *P. abelii* samples to the *P. abelii* centroid plus all of the *P. pygmaeus* samples to the *P. pygmaeus* centroid. The dotted line represents the distance of the *P. tapanuliensis* sample to the *P. abelii* centroid (exact permutation test; within-species distribution: p-value<0.001; between-species: p-value<0.001), whereas solid line represents the distance of the *P. tapanuliensis* samples to the *P. pygmaeus* centroid (within-species: p-value<0.001; between-species: p-value<0.001).

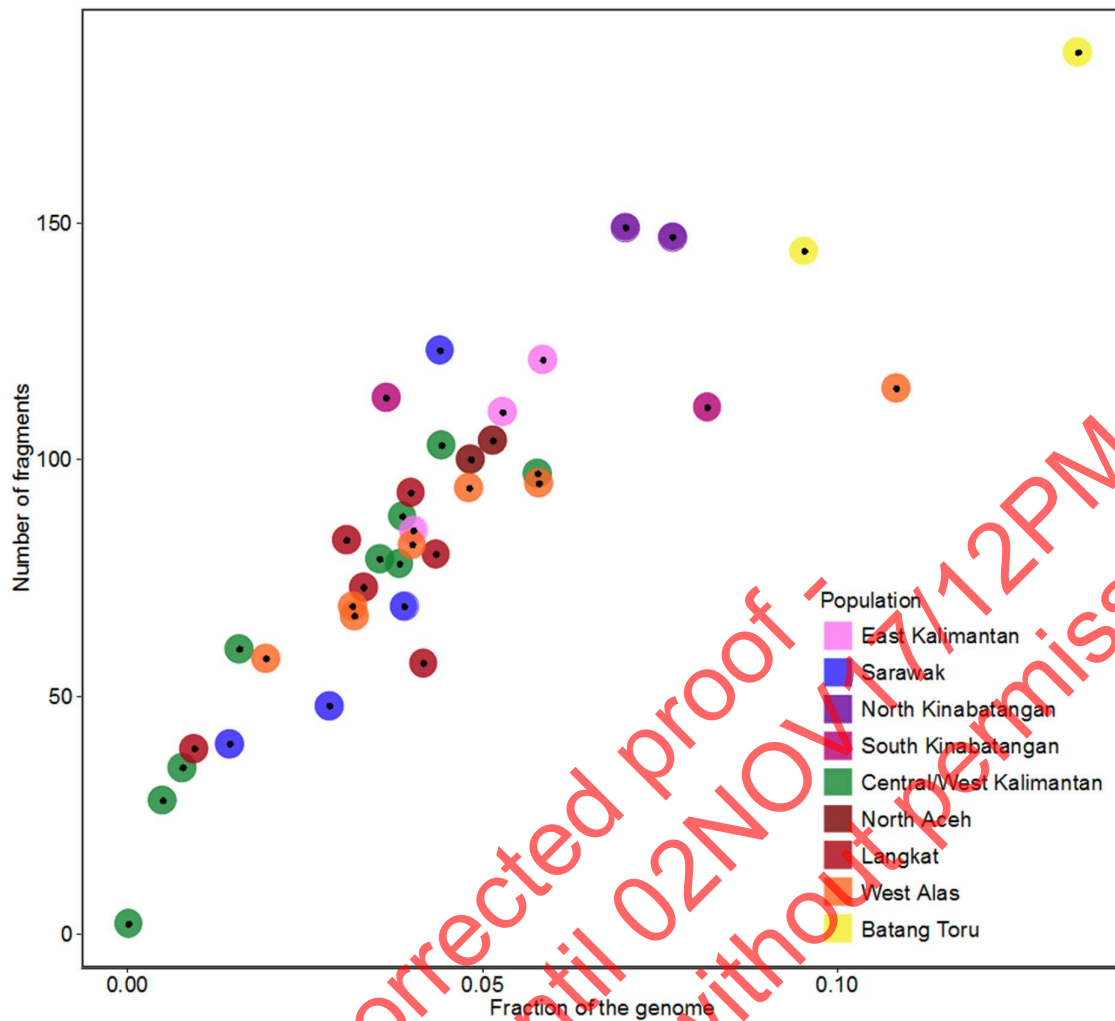


Figure S3. Signatures of recent inbreeding in different orangutan populations. Related to Figure 3C. Number of genomic fragments that are autozygous (y-axis) plotted against the total fraction of the genome covered by such fragments (x-axis). Each dot represents an individual, with sample origins represented by colors corresponding to those in Figure 2A.

Table S1. Summary statistics for the cranio-mandibular variables utilized in this study [mm]. Related to Figure 1B.

Species	PI	PN	NI	PO	LNS	BDS	MBA	MBP	BB	BOE	IB	OB	OH
<i>P. abelii</i>													
Mean	232.05	101.46	136.87	68.53	58.14	138.34	71.39	52.31	103.50	114.44	11.82	36.69	42.54
SD	13.27	10.18	7.10	3.12	4.63	6.79	4.08	4.26	4.32	8.45	1.45	1.74	5.09
Minimum	215.44	85.03	127.93	64.02	49.81	126.59	64.15	45.59	97.00	102.78	8.74	34.65	31.64
1st Quartile	222.07	95.77	130.99	66.31	55.71	134.18	68.89	50.13	101.00	106.96	11.25	35.16	41.50
Median	232.76	102.64	137.88	68.78	58.82	140.50	71.81	52.98	104.25	114.24	12.40	36.68	44.12
3rd Quartile	236.63	107.05	140.41	70.68	60.26	143.51	74.61	54.65	106.63	122.51	12.56	37.74	45.88
Maximum	256.78	116.77	149.32	72.38	64.68	145.59	76.21	58.97	109.00	124.82	13.29	39.48	46.89
n	8	8	8	8	8	8	8	8	8	8	8	8	8
<i>P. pygmaeus</i>													
Mean	234.36	104.80	138.45	64.29	57.58	144.23	71.25	53.64	110.66	115.05	12.23	35.91	41.43
SD	12.10	7.70	8.28	4.68	6.40	8.34	5.12	5.26	6.79	7.41	1.74	2.25	2.85
Minimum	211.58	88.18	120.58	55.50	47.55	128.18	55.69	39.28	98.50	98.01	8.99	29.67	35.29
1st Quartile	227.90	101.97	131.02	60.43	52.07	137.94	68.99	51.27	105.50	111.73	11.22	34.87	39.70
Median	237.86	106.15	138.84	65.09	59.53	146.10	72.25	54.77	111.00	116.28	11.91	35.49	41.66
3rd Quartile	243.66	109.74	146.17	66.83	61.77	148.50	74.43	56.91	114.50	120.32	13.22	36.88	43.32
Maximum	252.40	117.01	150.11	76.10	71.04	158.05	79.20	61.61	125.00	127.82	16.10	40.62	46.03
n	25	25	25	25	21	23	25	25	25	25	25	25	25
<i>P. tapanuliensis</i>													
Mean	224.72	90.80	139.54	69.85	70.52	136.52	65.00	59.94	101.50	120.00	12.42	33.80	33.38
n	1	1	1	1	1	1	1	1	1	1	1	1	1
Permutation tests													
vs. <i>P. abelii</i>	NS	NS	NS	NS	<0.001	NS	NS	NS	NS	NS	NS	NS	NS
vs. <i>P. pygmaeus</i>	NS	NS	NS	NS	0.048	NS	NS	NS	NS	NS	NS	NS	<0.001

PI = Prosthion-Inion Length, PN = Prosthion-Nasion Length, NI = Nasion-Inion Length, PO = Postorbital Breadth, LNS = Nuchal Surface Length, BDS = Nuchal Surface Breadth, MBA = Anterior Muzzle Breadth, MBP = Posterior Muzzle Breadth, BB = Braincase Breadth, BOE = Biorbital Breadth, IB = Interorbital Breadth, OB = Orbital Breadth, OH = Orbital Height.

Table S1 (continued). Summary statistics for the cranio-mandibular variables utilized in this study [mm]. Related to Figure 1B.

Species	DF	PB	PL	ProB	BZAE	ZAT	BT	TMB	TML	PPB	APB	LTTA	TMJA
<i>P. abelii</i>													
Mean	18.19	72.28	91.93	173.43	162.13	9.94	114.95	27.70	34.31	51.65	50.77	33.50	29.83
SD	3.12	3.77	8.70	10.85	6.58	1.50	4.02	2.22	2.75	1.29	3.30	1.19	1.49
Minimum	14.25	66.72	72.80	160.34	152.12	7.57	107.96	23.34	30.00	50.29	47.54	31.71	27.83
1st Quartile	15.41	70.10	91.05	164.82	158.83	9.09	113.07	26.66	32.50	50.63	48.91	32.83	28.43
Median	18.64	71.66	93.33	171.24	161.33	10.23	115.55	27.92	34.83	51.30	50.02	33.29	30.16
3rd Quartile	19.82	74.76	95.51	183.06	164.86	10.90	117.87	29.47	36.34	52.33	51.25	34.10	30.66
Maximum	22.63	78.24	101.29	188.43	174.36	12.06	119.69	30.00	37.77	54.08	58.17	35.24	31.90
n	8	8	8	8	8	8	8	8	8	8	8	8	8
<i>P. pygmaeus</i>													
Mean	14.30	73.59	91.82	171.85	166.19	8.61	119.93	25.67	31.38	49.45	50.08	33.90	31.27
SD	2.75	3.31	6.35	10.88	9.03	1.84	6.09	2.25	3.10	4.50	3.90	2.15	2.65
Minimum	8.39	66.33	80.07	148.42	146.44	3.89	109.33	21.32	25.38	43.87	43.01	28.40	24.68
1st Quartile	12.32	71.57	86.72	163.90	160.72	7.85	115.85	24.19	28.97	47.00	46.57	32.98	30.02
Median	14.75	74.33	92.48	174.43	168.50	8.62	118.83	25.72	31.35	48.20	51.18	34.10	31.78
3rd Quartile	15.70	75.62	96.37	179.31	174.05	9.72	123.81	27.29	33.60	49.90	52.43	35.35	33.12
Maximum	20.58	80.32	103.79	189.95	179.64	12.20	135.28	30.62	38.27	62.39	57.86	37.55	35.40
n	25	25	25	23	25	25	25	22	22	25	25	25.00	25.00
<i>P. tapanuliensis</i>													
n	6.04	73.37	82.40	164.30	160.46	10.38	109.48	23.17	29.20	33.78	33.71	23.93	22.46
n	1	1	1	1	1	1	1	1	1	1	1	1	1
Permutation tests													
vs. <i>P. abelii</i>	<0.001	NS	NS	NS	NS	NS	NS	NS	<0.001	<0.001	<0.001	<0.001	<0.001
vs. <i>P. pygmaeus</i>	<0.001	NS	NS	NS	NS	NS	NS	NS	NS	<0.001	<0.001	<0.001	<0.001

DF = Face Depth, PB = Palate Breadth, PL = Palate Length, ProB = Prosthion-Basion Length, BZAE = Bizygomatic Arch Breadth, ZAT = Zygomatic Arch Thickness, BT = Bitympanic Breadth, TMB = Foramen Magnum Breadth, TML = Foramen Magnum Length, PPB = Posterior Pterygoid Breadth, APB = Anterior Pterygoid Breadth, LTTA = Tympanic tube length, TMJA = Temporomandibular joint length.

Table S1 (continued). Summary statistics for the cranio-mandibular variables utilized in this study [mm]. Related to Figure 1B.

Species	BS	PM1M3A	MIB	MM1EB	RA	S	ITT	BiB	HLM	RWA	JIW	JM1EB	JPM1M3A
<i>P. abelii</i>													
Mean	80.41	55.19	39.85	72.01	109.36	61.79	42.11	131.63	159.06	60.55	30.06	59.81	65.99
SD	8.55	2.79	5.22	3.75	5.82	5.53	5.39	3.78	8.92	1.98	1.01	5.03	4.29
Minimum	70.92	50.96	30.12	66.65	102.21	53.71	36.14	127.16	146.64	58.26	28.49	49.03	60.80
1st Quartile	73.86	53.25	38.24	70.05	106.96	58.24	37.31	128.15	152.72	58.96	29.39	58.34	61.95
Median	78.89	55.66	41.21	71.39	107.57	60.92	41.83	131.22	156.98	60.19	30.07	61.08	68.43
3rd Quartile	86.83	57.13	43.22	73.67	110.56	65.51	45.66	134.72	167.33	61.86	30.87	62.35	68.86
Maximum	91.59	58.95	44.68	78.27	121.61	70.02	50.04	137.39	170.34	63.56	31.47	65.45	71.05
n	8	8	7	8	8	8	8	8	8	8	8	8	7
<i>P. pygmaeus</i>													
Mean	82.03	55.33	41.81	73.27	111.44	66.93	42.35	134.04	159.77	65.64	31.96	61.53	69.43
SD	7.32	3.16	2.54	3.45	5.99	5.00	3.25	11.28	12.60	5.22	2.94	3.71	3.26
Minimum	65.34	46.61	34.92	65.73	98.10	60.51	35.98	113.43	116.28	56.28	23.42	52.53	64.58
1st Quartile	78.24	53.99	40.65	71.19	109.16	63.35	40.56	126.02	155.88	63.06	30.60	60.31	67.35
Median	84.85	55.68	41.99	73.35	110.52	65.19	41.90	135.38	161.39	65.25	32.57	61.99	68.72
3rd Quartile	88.18	57.79	43.77	75.48	113.57	70.80	43.68	142.78	166.15	67.96	33.41	64.02	71.65
Maximum	90.93	60.46	45.03	80.25	124.63	79.08	49.32	154.99	180.02	78.90	37.85	66.82	75.85
n	23	24	25	25	20	21	21	21	21	21	21	21	21
<i>P. tapanuliensis</i>													
	77.83	55.27	28.31	62.66	113.61	49.29	31.80	119.98	150.58	55.94	24.44	55.32	70.00
n	1	1	1	1	1	1	1	1	1	1	1	1	1
Permutation tests													
vs. <i>P. abelii</i>	NS	NS	<0.001	<0.001	NS	<0.001	<0.001	<0.001	NS	<0.001	<0.001	NS	NS
vs. <i>P. pygmaeus</i>	NS	NS	<0.001	<0.001	NS	<0.001	<0.001	NS	NS	NS	0.048	NS	NS

BS = Basion-Staphylion Length, PM1M3A = Maxillary Length of PM1-M3, MIB = Maxillary Incisor Complex Breadth, MM1EB = External Breadth of the Maxilla at M1, RA = Ramus Height, S = Symphysis Length, ITT = Inferior transverse torus, BiB = Bicondylar Breadth, HLM = Horizontal Length, RWA = Ramus Width, JIW = Mandibular Incisor Complex Breadth, JM1EB = External Breadth of the Mandible at M1, JPM1M3A = Mandibular Length of PM1-M3.

Table S2. Summary statistics for the dental variables utilized in this study [mm]. Related to Figure 1B.

Species	UCB	LCB	LM1L	LM1B	LM1A
<i>P. abelii</i>					
Mean	17.90	15.96	13.12	10.81	141.86
SD	1.77	0.96	0.57	0.60	10.23
Minimum	15.67	14.34	12.48	10.08	128.51
1st Quartile	16.76	15.61	12.66	10.36	133.35
Median	17.37	16.05	13.00	10.87	145.43
3rd Quartile	19.38	16.29	13.56	11.18	148.32
Maximum	20.54	17.55	13.89	11.68	155.74
n	8	8	7	7	7
<i>P. pygmaeus</i>					
Mean	18.08	17.03	13.46	11.22	151.04
SD	1.57	1.61	0.78	0.70	13.58
Minimum	14.82	14.46	11.38	10.11	126.17
1st Quartile	17.37	15.59	13.17	10.57	140.12
Median	17.85	17.20	13.50	11.31	147.79
3rd Quartile	19.27	18.27	13.83	11.74	162.36
Maximum	20.86	19.60	15.01	12.45	171.56
n	19	19	20	20	20
<i>P. p. palaeosumatrensis</i>					
Mean	20.94	17.28	14.99	13.05	195.71
SD	1.91	1.47	0.53	0.58	14.09
Minimum	18.30	15.30	14.00	12.10	175.45
1st Quartile	19.10	16.05	14.60	12.70	183.80
Median	21.20	17.00	14.90	13.00	193.50
3rd Quartile	22.00	18.15	15.40	13.48	205.74
Maximum	24.60	20.50	16.20	14.50	234.90
n	21	39	90	90	90
<i>P. tapanuliensis</i>					
Mean	21.50	19.44	13.65	11.37	155.20
n	1	1	1	1	1
Permutation tests					
vs. <i>P. abelii</i>	<0.001	<0.001	NS	NS	NS
vs. <i>P. pygmaeus</i>	NS	NS	NS	NS	NS
vs. <i>P. p. palaeosumatrensis</i>	NS	NS	<0.001	<0.001	<0.001

UCB = Upper canine breadth, LCB = Lower canine breadth, LM1L = Lower M1 length, LM1B = Lower M1 breadth, LM1A = Lower M1 area.

Table S3. Summary statistics for the 15 long call variables utilized in this study. Related to STAR Methods.

Species	No. of pulses	Call Dur [s]	Sound Dur [s]	Interval Dur [s]	Max Freq R [Hz]
<i>P. abelii</i>					
Mean	40.74	72.70	0.61	1.09	558.83
SD	9.63	24.17	0.08	0.19	121.73
Minimum	26.50	46.22	0.47	0.76	369.76
1st Quartile	32.94	50.42	0.57	0.98	468.26
Median	38.75	65.20	0.61	1.12	557.78
3rd Quartile	47.67	96.25	0.67	1.22	642.11
Maximum	56.50	113.60	0.74	1.46	746.86
n	14	14	14	14	14
<i>P. pygmaeus</i>					
Mean	25.41	53.59	0.69	1.37	706.99
SD	7.72	13.73	0.18	0.34	184.11
Minimum	10.00	28.76	0.43	0.80	257.25
1st Quartile	21.00	45.79	0.57	1.06	621.98
Median	25.00	51.80	0.66	1.39	689.88
3rd Quartile	29.00	60.68	0.79	1.63	836.52
Maximum	45.00	89.36	1.28	1.97	998.74
n	29	29	29	29	27
<i>P. tapanuliensis</i>					
Mean	57.11	112.06	0.66	1.06	830.64
SD	5.97	0.39	0.04	0.06	42.15
Minimum	52.89	111.78	0.63	1.02	800.84
1st Quartile	55.00	111.92	0.64	1.04	815.74
Median	57.11	112.06	0.66	1.06	830.64
3rd Quartile	59.22	112.19	0.67	1.08	845.55
Maximum	61.33	112.33	0.68	1.10	860.45
n	2	2	2	2	2
Permutation tests					
vs. <i>P. abelii</i>	NS	NS	NS	NS	<0.001
vs. <i>P. pygmaeus</i>	<0.001	NS	NS	NS	NS

No. of pulses = Number of pulses, Call Dur = Duration of call, Sound Dur = Duration of sound, Interval Dur = Duration of interval, Max Freq R = Maximum frequency of roar (R) pulse type.

Table S3 (continued). Summary statistics for the 15 long call variables utilized in this study. Related to STAR Methods.

Species	Min Freq R [Hz]	Peak Freq R [Hz]	Shape R [Hz/s]	Freq Max [Hz]	Freq Min [Hz]
<i>P. abelii</i>					
Mean	141.77	310.61	709.07	824.29	64.04
SD	39.16	60.44	155.29	193.91	30.40
Minimum	88.90	186.82	450.06	460.38	17.64
1st Quartile	103.36	279.97	572.28	732.78	49.39
Median	148.70	294.25	739.86	837.01	61.87
3rd Quartile	173.99	362.27	833.23	948.13	75.76
Maximum	200.53	400.52	934.08	1111.25	145.50
n	14	14	14	14	14
<i>P. pygmaeus</i>					
Mean	177.36	403.82	749.46	984.66	62.13
SD	61.70	111.90	247.91	291.69	29.46
Minimum	74.08	202.17	230.78	354.29	10.58
1st Quartile	135.31	336.22	642.39	896.06	45.86
Median	173.87	387.60	730.15	977.19	57.00
3rd Quartile	215.93	436.23	870.72	1167.10	77.16
Maximum	361.07	732.13	1372.05	1498.60	144.44
n	27	27	27	29	29
<i>P. tapanuliensis</i>					
Mean	199.17	399.56	1036.53	1136.15	87.69
SD	7.57	19.16	118.19	128.95	10.08
Minimum	193.82	386.02	952.96	1044.97	80.57
1st Quartile	196.50	392.79	994.74	1090.56	84.13
Median	199.17	399.56	1036.53	1136.15	87.69
3rd Quartile	201.85	406.33	1078.31	1181.74	91.26
Maximum	204.53	413.11	1120.10	1227.33	94.82
n	2	2	2	2	2
Permutation tests					
vs. <i>P. abelii</i>	NS	NS	<0.001	NS	NS
vs. <i>P. pygmaeus</i>	NS	NS	NS	NS	NS

Min Freq R = Minimum frequency of roar (R) pulse type, Peak Freq R = Peak frequency of roar pulse type, Shape R = Average shape of roar pulse type, Freq Max = Maximum frequency of call, Freq Min = Minimum frequency of call.

Table S3 (continued). Summary statistics for the 15 long call variables utilized in this study. Related to STAR Methods.

Species	Rate [pulses/20s]	Huitus [%]	Roar [%]	Sigh [%]	Intermediary [%]
<i>P. abelii</i>					
Mean	0.81	10.26	54.57	6.54	5.31
SD	0.11	13.68	15.66	4.29	5.41
Minimum	0.62	0.00	19.35	0.00	0.00
1st Quartile	0.72	3.15	48.03	5.44	1.10
Median	0.81	5.61	53.85	6.84	4.83
3rd Quartile	0.89	8.68	66.53	8.23	6.96
Maximum	0.97	48.39	75.76	13.51	16.67
n	14	14	14	14	14
<i>P. pygmaeus</i>					
Mean	0.52	16.26	28.36	15.51	11.02
SD	0.13	15.58	17.23	18.17	9.26
Minimum	0.30	0.00	0.00	0.00	0.00
1st Quartile	0.45	0.00	20.29	4.35	4.35
Median	0.48	16.54	26.92	8.00	8.21
3rd Quartile	0.64	23.11	35.55	20.30	15.38
Maximum	0.79	64.00	80.95	80.00	41.67
n	29	29	29	29	29
<i>P. tapanuliensis</i>					
Mean	0.88	7.80	39.58	20.47	1.98
SD	0.08	11.03	0.81	10.24	2.80
Minimum	0.82	0.00	39.01	13.23	0.00
1st Quartile	0.85	3.90	39.29	16.85	0.99
Median	0.88	7.80	39.58	20.47	1.98
3rd Quartile	0.91	11.69	39.87	24.09	2.97
Maximum	0.93	15.59	40.15	27.71	3.96
n	2	2	2	2	2
Permutation tests					
vs. <i>P. abelii</i>	NS	NS	NS	<0.001	NS
vs. <i>P. pygmaeus</i>	<0.001	NS	NS	NS	NS

Rate = Number of pulses per 20 s, Huitus = Percent number of huitus (H) pulse type, Roar = Percent number of roar (R) pulse type, Sigh = Percent number of sigh (S) pulse type, Intermediary = Percent number of intermediary (I) pulse type.

Table S4. Details of study individuals. Related to Figure 2A.

Species	Sampling area	Individual ID	Name	Sex	Depth ^a	Source	Comments and origin details, if available
<i>P. abelii</i>	Langkat	PA_KB4661	Bubbles	M	4.76	[S1]	Wild-born
<i>P. abelii</i>	Langkat	PA_KB5883	Sibu	M	4.99	[S1]	Wild-born
<i>P. abelii</i>	Langkat	PA_A947	Elsi	F	27.39	[S2]	Wild-born
<i>P. abelii</i>	Langkat	PA_A948	Kiki	F	23.71	[S2]	Wild-born
<i>P. abelii</i>	Langkat	PA_A950	Babu	F	26.28	[S2]	Wild-born
<i>P. abelii</i>	Langkat	PA_A952	Buschi	M	21.03	[S2]	Wild-born
<i>P. abelii</i>	North Aceh	PA_A949	Dunja	F	27.39	[S2]	1 st Generation by 456 and 457 both wild-born Sumatra
<i>P. abelii</i>	North Aceh	PA_B018	Jeff	M	16.31	This study	Wild-born; Desa Seuneubok Bayu, Indra Makmu district
<i>P. abelii</i>	West Alas	PA_KB4361	Likoe	F	5.66	[S1]	Wild-born
<i>P. abelii</i>	West Alas	PA_SB550	Doris	F	4.86	[S1]	Wild-born
<i>P. abelii</i>	West Alas	PA_B017	Miky	F	13.74	This study	Wild-born; Aluebillie, Aceh Nagan Raya, Aceh province
<i>P. abelii</i>	West Alas	PA_A953	Vicky	F	17.78	This study	Wild-born
<i>P. abelii</i>	West Alas	PA_A955	Suma	F	25.27	This study	Wild-born
<i>P. abelii</i>	West Alas	PA_A964	Rochelle	F	11.06	This study	Wild-born
<i>P. abelii</i>	West Alas	PA_B020	Maini	F	16.3	This study	Wild-born; Aceh Sealatan near Suaq Balimbing
<i>P. tapanuliensis</i>	Batang Toru	PA_KB9258	Baldy	F	5.79	[S1]	Wild-born
<i>P. tapanuliensis</i>	Batang Toru	PA_KB9258	Baldy	F	5.79	[S1]	Wild-born

^amean effective whole-genome sequencing coverage (estimated from the quality filtered BAM files).

Table S4 (continued). Details of study individuals. Related to Figure 2A.

Species	Sampling area	Individual ID	Name	Sex	Depth ^a	Source	Comments and origin details, if available
<i>P. pygmaeus</i>	Central Kalimantan	PP_KB4204	Dolly	M	5.61	[S1]	Wild-born
<i>P. pygmaeus</i>	Central Kalimantan	PP_KB5404	Billy	F	12.24	[S1]	Wild-born
<i>P. pygmaeus</i>	Central Kalimantan	PP_KB5405	Dennis	M	5.61	[S1]	Wild-born
<i>P. pygmaeus</i>	Central Kalimantan	PP_A940	Temmy	F	21.8	[S2]	1 st Generation by 793 and 794 both wild-born Borneo
<i>P. pygmaeus</i>	Central Kalimantan	PP_A941	Sari	F	23.17	[S2]	1. Gen. by 202 and 322 both wild-born Borneo
<i>P. pygmaeus</i>	Central Kalimantan	PP_A943	Tilda	F	24.17	[S2]	Wild-born
<i>P. pygmaeus</i>	Central Kalimantan	PP_A944	Napoleon	M	23.32	[S2]	Wild-born
<i>P. pygmaeus</i>	Central Kalimantan	PP_A938	Lotti	F	18.62	This study	1 st Generation by 358 and 422 both wild-born Borneo
<i>P. pygmaeus</i>	West Kalimantan	PP_A983	Claus	M	29.71	This study	Wild-born; Pontianak
<i>P. pygmaeus</i>	East Kalimantan	PP_KB5543	Louis	M	6.03	[S1]	Wild-born
<i>P. pygmaeus</i>	East Kalimantan	PP_A984	Barong	F	29.89	This study	Wild-born; Taman Nasional Kutai
<i>P. pygmaeus</i>	East Kalimantan	PP_A985	Panjul	M	30.13	This study	Wild-born; Taman Nasional Kutai
<i>P. pygmaeus</i>	North Kinabatangan	PP_A987	Tara	F	30.65	This study	Wild-born; Bukit Garam, Kinabatangan area
<i>P. pygmaeus</i>	North Kinabatangan	PP_A988	Kala	M	31.06	This study	Wild-born; Kg. Tikolod, Tambunan
<i>P. pygmaeus</i>	South Kinabatangan	PP_5062	Ampal	M	13.81	This study	Wild-born; Lahad Datu, Kinabatangan area
<i>P. pygmaeus</i>	South Kinabatangan	PP_A989	Micelle	F	27.3	This study	Wild-born; Lahad Datu, Kinabatangan area
<i>P. pygmaeus</i>	Sarawak	PP_KB5406	Dinah	F	4.9	[S1]	Wild-born
<i>P. pygmaeus</i>	Sarawak	PP_A939	Nonja	F	20.48	[S2]	1 st Generation by 1052 and 1012 both from Sarawak
<i>P. pygmaeus</i>	Sarawak	PP_A942	Gusti	F	23.12	This study	1 st Generation by 1435 and 1392 both wild-born Borneo
<i>P. pygmaeus</i>	Sarawak	PP_A946	Kajan	M	22.39	This study	Wild-born

^amean effective whole-genome sequencing coverage (estimated from the quality filtered BAM files).

Table S5. Parameter estimation of the best supported models in the ABC and G-PhoCS analyses. Related to Figure 3B.

<i>ABC</i>				
Parameter^a	Prior distribution	Mode	Mean	95%-HPD^b
N _{NOW} BO (4)	loguniform (300–32,000)	1,487	1,759	407–8,002
N _{NOW} NT (2)	loguniform (300–32,000)	2,854	3,212	517–21,691
N _{STRUC} NT (2)	loguniform (3,000–320,000)	19,925	26,795	3,736–197,419
N _{NOW} ST	loguniform (300–32,000)	2,520	2,429	524–10756
N _{ANC} ST	loguniform (1,000–100,000)	35,874	28,907	7,522–99,885
N _{BN} BO	loguniform (300–32,000)	4,473	3,719	523–27,948
N _{ANC} BO	loguniform (3,000–320,000)	30,655	36,257	5,924–266,244
N _{ANC} NT	loguniform (1,000–100,000)	53,811	29,654	5,115–99,885
T _{BNEND} BO	uniform (8,750–400,000)	71,969	125,689	8,848–272,775
T _{BNDUR} BO	uniform (250–100,000)	33,583	46,508	924–92,087
T _{SPLIT} BO	uniform (400,000–1,500,000)	674,055	681,760	427,878–921,400
T _{SPLIT} NT	uniform (1,500,000–4,000,000)	3,382,200	2,827,150	1,712,005–3,977,250
T _{DEC} NT	uniform (250–100,000)	82,635	54,372	10,126–99,975
T _{STRUC} NT	uniform (100,000–1,500,000)	1,057,388	873,195	241,301–1,499,650
T _{MIGSTOP}	uniform (8,750–400,000)	303,118	253,968	82,680–399,903
N _m WBO	loguniform (0.030–32.000)	6.818	1.272	0.060–31.568
N _m WNT	loguniform (0.030–32.000)	0.128	0.594	0.032–14.973
N _m BOST	loguniform (0.003–3.200)	0.016	0.021	0.003–0.127
N _m STBO	loguniform (0.003–3.200)	0.003	0.007	0.003–0.021
N _m NTST	loguniform (0.010–10.000)	0.294	0.228	0.019–2.116
N _m STNT	loguniform (0.010–10.000)	0.86	0.687	0.058–9.166

^a, BO = Borneo, NT = Sumatra north of Lake Toba, ST = Sumatra south of Lake Toba, N_{NOW} = current effective population size (N_e), N_{BN} = N_e during population bottleneck, N_{ANC} = ancestral N_e, N_{STRUC} = N_e before recent decline (number of populations of this size), T_{BNEND} = time since population bottleneck ended, T_{BNDUR} = duration of bottleneck, T_{SPLIT} = population split time, T_{DEC} = time since population decline, T_{STRUC} = time since establishment of population structure, T_{MIGSTOP} = time since migration between BO and ST stopped (all times were converted to years assuming a generation time of 25 years), N_mWBO = number of migrants per generation among populations on Borneo, N_mWNT = number of migrants among populations north of Lake Toba, N_mXY = number of migrants in X from Y; ^b, 95%-highest posterior density interval.

Table S5 (continued). Parameter estimation of the best supported models in the ABC and G-PhoCS analyses. Related to Figure 3B.

<i>G-PhoCS</i>				
Parameter ^a	Prior distribution ^b	Mode	Mean	95%-HPD ^c
N _{NOW} BO	Gamma ($\alpha=1$; $\beta=500$)	17,939	17,992	17,655–18,338
N _{NOW} NT	Gamma ($\alpha=1$; $\beta=500$)	16,123	16,114	15,588–16,655
N _{NOW} ST	Gamma ($\alpha=1$; $\beta=500$)	26,787	26,791	26,113–27,477
N _{ANC} BOST	Gamma ($\alpha=1$; $\beta=500$)	114,303	114,451	110,626–118,704
N _{ANC} PONGO	Gamma ($\alpha=1$; $\beta=500$)	33,162	33,223	32,316–34,119
T _{SPLIT} BOST	Gamma ($\alpha=1$; $\beta=2000$)	575,551	578,150	563,217–593,200
T _{SPLIT} PONGO	Gamma ($\alpha=1$; $\beta=500$)	2,273,045	2,278,133	2,208,383–2,351,917
m_BO->ST	Gamma ($\alpha=0.002$; $\beta=0.00001$)	4.45×10^{-6}	4.45×10^{-6}	$4.08-4.80 \times 10^{-6}$
m_ST->BO	Gamma ($\alpha=0.002$; $\beta=0.00001$)	1.17×10^{-6}	1.20×10^{-6}	$0.95-1.46 \times 10^{-6}$
m_NT->ST	Gamma ($\alpha=0.002$; $\beta=0.00001$)	3.19×10^{-6}	3.27×10^{-6}	$2.55-3.94 \times 10^{-6}$
m_ST->NT	Gamma ($\alpha=0.002$; $\beta=0.00001$)	8.28×10^{-5}	8.29×10^{-5}	$7.98-8.60 \times 10^{-5}$
m_BOST->NT	Gamma ($\alpha=0.002$; $\beta=0.00001$)	8.39×10^{-5}	8.53×10^{-5}	$5.47-11.44 \times 10^{-5}$
m_NT->BOST	Gamma ($\alpha=0.002$; $\beta=0.00001$)	6.87×10^{-12}	2.18×10^{-10}	$0.0015-11.73 \times 10^{-10}$

^a, BO = Borneo, NT = Sumatra north of Lake Toba, ST = Sumatra south of Lake Toba, BOST = ancestral population of BO and ST, PONGO = ancestral population of all orangutans, N_{NOW} = current effective population size, N_{ANC} = ancestral effective population size, T_{DIV} = population split time in years, m_X->Y = migration rate per generation from X to Y forward in time; ^b, prior distribution of mutation-scaled parameters; ^c, 95%-highest posterior density interval. All scaled estimates from G-PhoCS were converted to absolute values assuming a mutation rate of 1.5×10^{-8} mutations per base pair per generation and a generation time of 25 years.

Table S6. PCR primers for Sanger sequencing of mitogenomes. Related to STAR Methods.

Primer name	Primer sequence (5'-3')	Primer position^a
F1	GYTTGGTCCTRGCCTTTC	77
R1	AGTACRCTTACCATGTTAC	1004
F2	ACACACCGCCCGTCAC	902
R2	CAGGTCAATTTCACTGGT	2109
F3	CATCACCTCTAGCATTAC	1931
R3	ATTAGGGCGTAGTTWGAG	3120
F4	AAGATGGCAGAGCCCG	2658
R4	CAACATTTTCGGGGTATG	3874
F5	CTGACRAAAGAGTTACTTTG	3698
R5	GGGCTTAGCTTAATTAAG	5076
F6	CCAAGAGCCTTCAAAGC	4958
R6	CYGTRAATATRTGGTGGGC	6224
F7	TWCTCYCACCCAGGAGC	5732
R7	GGGGYTGGCTTGAACCC	6917
F8	AAAGGAAGGAATCGAACC	6873
R8	GTCTTTAACTTAAAAGTTAA	7776
F9	GAGGCCCAYTGCAAAGC	7729
R9	TGGTGGCCTTGGTATGT	8858
F10	CYACCCARCTWTCCATAAA	8250
R10	CCTCATCAGTAGATGGAG	9425
F11	TTCCACGGCCTCCACG	9253
R11	GATAAGGGGTCGGAGG	10384
F12	AAAYAAATGATTTGACTCAT	9863
R12	AAGCTTCAGGGGGTTG	11125
F13	CGACAAACAGAYCTAAAATC	11047
R13	GTTGATRRTTGGGTCTGAG	12135
F14	GTGCAACTCCAAATAAAAG	11770
R14	AGGGCTCAGGCGTTGG	13016
F15	TCTGCACCCAYGCCTTC	12776
R15	GTATGATGGTTGTTTTTGG	13943
F16	GCACCCGCACCAATAG	13687
R16	GGCCTCAYGGGAGGAC	14609
F17	CGAGAYGTAAACTACGGC	14411
R17	AGTTAAGTRCTTTTTCTCTG	15435
F18	CAAGCAACAGAGCATAAC	15130
R18	TGTCTTATTTAAGGGGAAC	16017
F19	CTGTATCCGGCATCTGG	15943
R19	CGCGGTGGCTGGCAC	324

^a, Sequence positions (5'-end) on the *Pongo abelii* reference mitochondrial genome NC_002083.

Supplemental References

- S1. Locke, D.P., Hillier, L.W., Warren, W.C., Worley, K.C., Nazareth, L.V., Muzny, D.M., Yang, S.-P., Wang, Z., Chinwalla, A.T., Minx, P., et al. (2011). Comparative and demographic analysis of orang-utan genomes. *Nature* 469, 529-533.
- S2. Prado-Martinez, J., Sudmant, P.H., Kidd, J.M., Li, H., Kelley, J.L., Lorente-Galdos, B., Veeramah, K.R., Woerner, A.E., O'Connor, T.D., Santpere, G., et al. (2013). Great ape genetic diversity and population history. *Nature* 499, 471-475.

Uncorrected proof -
Under embargo until 02NOV17/12PM ET
-Do not distribute without permission-